Degradation and Stabilization of Perovskite Inks for Solar Cells

by

Sean Bernard Reinecke

B.Sc., University of Victoria, 2022

A Thesis Submitted in Partial Fulfillment of the

Requirements for the Degree of

MASTER OF SCIENCE

in the Department of Chemistry

Supervisory Committee

Dr. Makhsud I. Saidaminov, Supervisor

(Department of Electrical and Computer Engineering)

Dr. Jeremy E. Wulff, Departmental Member

(Department of Chemistry)

Dr. Samira Gharehkhani, Outside Member

(Department of Electrical and Computer Engineering)

Abstract

A photovoltaic cell (PV) converts photonic energy into an electrical current. A typical photovoltaic cell is a multilayer device consisting of an absorber layer, hole transporter layer (HTL), electron transporter layer (ETL), a transparent electrode and a back electrode. These devices are capable of directly translating a portion of the vast amounts of solar energy that collide with the Earth into usable electrical energy. Presently the vast majority of these devices use silicon for the absorber layer and positively or negatively doped silicon for the two charge carrier transport layers. The cost of manufacturing solar panels has dropped dramatically in the past decades, leading to their widespread adoption.

However, silicon is limited by its high manufacturing cost and indirect bandgap (the energetic and momentum difference between the valence band and conduction band in a semiconductor). Thus, there is a hunt for new semiconductor materials that do not possess the same intractable issues as silicon. One very promising emergent material is perovskite. Perovskite solar cells (PSCs) possess a number of advantages over traditional silicon devices. They can be deposited using standard wet chemical techniques and equipment, they require far lower processing energy, and they can be made thin enough to form flexible devices. These devices have seen dramatic improvement in efficiency over the few years.

Unfortunately, these devices are presently too unstable under ambient conditions for widespread adoption. They react rapidly with moisture and oxygen in the air. Formamidinium lead iodide, the highest performing variant of perovskite used in solar cells, have an unstable crystal structure at room temperature. Not only is the device unstable, but so is the ink used to deposit the solar absorbent layer.

Perovskite precursor inks suffer various forms of degradation, such as iodide anion oxidation and organic cation breakdown, hindering reliable perovskite solar cell manufacturing. This thesis will show that benzylhydrazine hydrochloride (BHC) not only retards the buildup of iodine as previously reported but also prevents the breakdown of organic cations. Through investigating BHC and iodine chemical reactions, we

elucidate protonation and dehydration mechanisms, converting BHC to harmless volatile compounds, thus preserving perovskite film crystallization and solar cell performance. This inhibition effect lasts nearly a month with minimal BHC, in contrast with control inks where organic cations fully react in less than a week. This enhanced understanding, from additive stabilization to end products, promises improved perovskite solar cell production reliability.

The thesis consists of 4 chapters:

- Chapter 1 will introduce the fundamentals (structure and optoelectronic properties) of perovskite solar cells. In addition, the objectives of the thesis will be discussed at the end of this chapter.
- Chapter 2 gives an overview of the methodology used in the course of my research and images of relevant devices.
- Chapter 3 contains the results of the research and its analysis focusing on the use of, and understanding of, BHC as a stabilizer.
- Chapter 4 is a conclusion and overview of future prospective research.

Table of Contents

Table of Figures

List of Abbreviations

MA – methylammonium

FA – formamidinium

Pb – lead

BHC – benzylhydrazine hydrochloride

DMF – dimethylformamide

DMSO – dimethyl sulfoxide

NMP – *N*-methyl-2-pyrrolidone

2ME – 2-methoxy-ethanol

IPA – isopropyl alcohol

MACl – methylammonium chloride

MFA+ – methyl formamidinium

PV – photovoltaic device

PSC – perovskite solar cells

V_{OC} – open-circuit voltage

J_{SC} – short-circuit current

FF – fill factor

PCE – power conversion efficiency

EQE – external quantum efficiency

ITO – indium-doped tin oxide

PCS – perovskite solar cell

XRD – X-ray diffraction

SEM – scanning electron microscopy

NMR – nuclear magnetic resonance

HSQC – heteronuclear single quantum coherence

HMBC – heteronuclear multiple quantum coherence

NIP – negative-intrinsic-positive device

PIN – inverted or positive-intrinsic-negative

HTL – hole transport layer

ETL – electron transport layer

Acknowledgments

I thank Dr. Makhsud I. Saidaminov for his supervision over the course of this project. I also thank Dr. Jeremy E. Wulff and Dr. Chris Barr for their mentorship. My appreciation also goes out to my colleagues in the Saidaminov group whose support, both practical and personal, has done so much for me.

I would also like to thank Solaires Entreprises Inc. and Canada's Natural Sciences and Engineering Research Council (ALLRP 561355-20) for their financial support to execute my projects. As well as the Canadian Foundation for Innovation (40326) and B.C. Knowledge Development Fund (806169) for support in acquisition of infrastructure used in my projects.

Chapter 1. Introduction

1-1. Abstract

The development of commercially viable solar power relies on affordable, mass producible and reliable semiconductor materials. Perovskites are a novel semiconductor material that show much promise due to its ease of manufacture, direct bandgap, high charge carrier mobility, bandgap tunability and elemental abundance.[1] However, there are several barriers to industry level upscaling; most notably, the relative instability of both the devices and the precursor inks used in their manufacture.[2,3] Perovskite precursor inks suffer various forms of degradation, such as iodide anion oxidation and organic cation breakdown, complicating perovskite solar cell manufacturing.[4] This chapter aims to explain the basics of perovskites, their use in solar cells and the issues preventing their widespread industrial applications.

1-2. Perovskites and their structure

Perovskites are a class of mineral that share a similar structure to, and are named after, perovskite ($CaTiO_3$).[5]. This mineral was itself named after the Russian minerologist Lev Perovski. Their general formula is ABX_3, with A being a cation with oxidation state 1+; B a cation with oxidation state 2+; and X is anionic with oxidation state 1−.[5] A subcategory of perovskites are metal-halide hybrid organic-inorganic perovskites which consist of a system of corner-sharing BX_6 octahedra, with A filling a hole in the cuboctahedral lattice formed by the surrounding 12 X atoms.[6] B is typically a metal in a 2+ oxidation state, X is a halide in a 1- oxidation state and A is a cation of the correct size for the cuboctahedral hole that it occupies and the 1+ oxidation state required to ionically balance the mineral.[7] See Figure 1-1 for a graphical representation.

From the size limitations for A comes the formula for the Goldschmidt tolerance factor $(t), t = \frac{rA+rX}{\sqrt{2}(rB+rX)}$ where t must be between 0.8 and 1.0 for a stable crystal structure.[8] For this thesis the focus shall

be on formamidium, lead, halides, as the A-B-Xs respectively. Although, it is acknowledged that there are a numerous other combinations that fit the requirements.

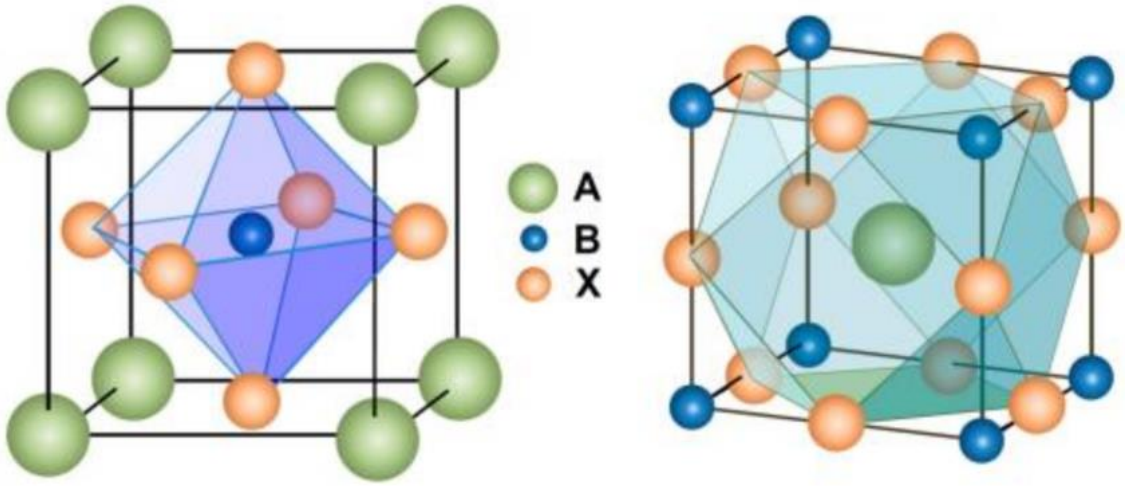

Figure 1-1. Idealized perovskite crystal lattice (left panel) showing BX_6 octahedral and (right panel) AX_{12} cuboctahedral geometry. Reprinted figure with permission from [6] Copyright (2017) by the American Physical Society.

1-3. Perovskite solar cells

Solar power is a promising long-term solution to the ongoing energy crisis. However, the current well-developed commercial form of solar panels relies on silicon which has a variety of issues including low defect tolerance, high energy input of manufacturing and an indirect bandgap.[9] Due to the high manufacturing cost of electronics grade silicon semiconductors, there is something of a lower limit to the cost of these devices.[10] This cost is material specific and unavoidable. Silicon based solar panels require extremely strict production conditions necessitated by the low defect tolerance of the material and the high energy input needed due to the high melting point of silicon.[11] Additionally, silicon possesses an indirect bandgap which dramatically increases the thickness required to efficiently absorb light.[9] While much can and has been done to improve industrial production of these devices, with the energy payback time being

theoretically lowered to 2.3 years for devices with a 30-year lifespan[12], the fundamental nature of silicon cannot be overcome.

These issues compound with each other. The low defect tolerance of electronic quality silicon necessitates incredibly demanding manufacturing conditions, under which the silicon must be heated to extreme temperatures for processing into films, and the indirect bandgap requires a thick absorber layer of this expensive material. Thus, there is a need for superior solar absorber materials. Figure 1-3 shows the development of many different solar cell architectures. Perovskite solar cells (PSCs) have shown a remarkable improvement since their discovery; going from 3.8% percent power conversion (PCE) in 2009 to a verified value of 26.1%.

PSCs consist of a perovskite light absorber layer sandwiched between a negative electron transport layer and a positive hole transport layer. When the absorber layer is struck with light of greater energy than the bandgap, an electron is excited from the valence band to the conduction band, with a corresponding positively charged region, or hole, being left behind. Due to this, hole-electron pairs are siphoned off by the positive and negatively charged transport materials, creating an electrical current. Solar cells possess either a negative-intrinsic-positive (NIP) or an inverted positive-intrinsic-negative (PIN) architecture (Figure 1-2). There exist myriad options for all three layers, dependant upon the required bandgap alignment.

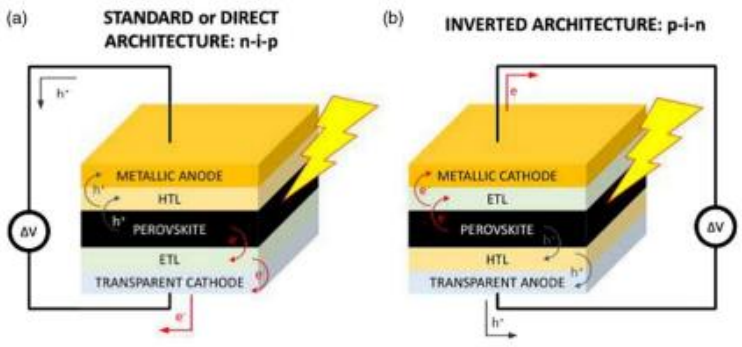

Figure 1-2. Schematic of (a) standard NIP and (b) inverted PIN perovskite solar cells. Reprinted from [13] an open access article.

To characterize the performance of solar cells, they are placed under a standardized light source, also called 1 sun with a power input of P_{in}=100 mW/cm^2. Then the cell is applied voltage and the produced current is measured, obtaining a current-voltage (J-V) characteristic of the device. From the resultant J-V graph, the open current voltage, V_{oc} (i.e., J-V intercept with voltage axis), and short circuit current, J_{sc} (i.e., J-V intercept with current axis) can be identified. The fill factor (FF) or ideality factor can be quantified by identifying the point on the graph of maximum power, creating a square with that point and the axes, then comparing that area to the area defined by J_{sc} and V_{oc}. The power conversion efficiency (PCE%) can thus be calculated using these values with this formula: $PCE(\%) = J_{sc} \cdot V_{oc} \cdot FF\% / P_{in}$, where P_{in} is power input.

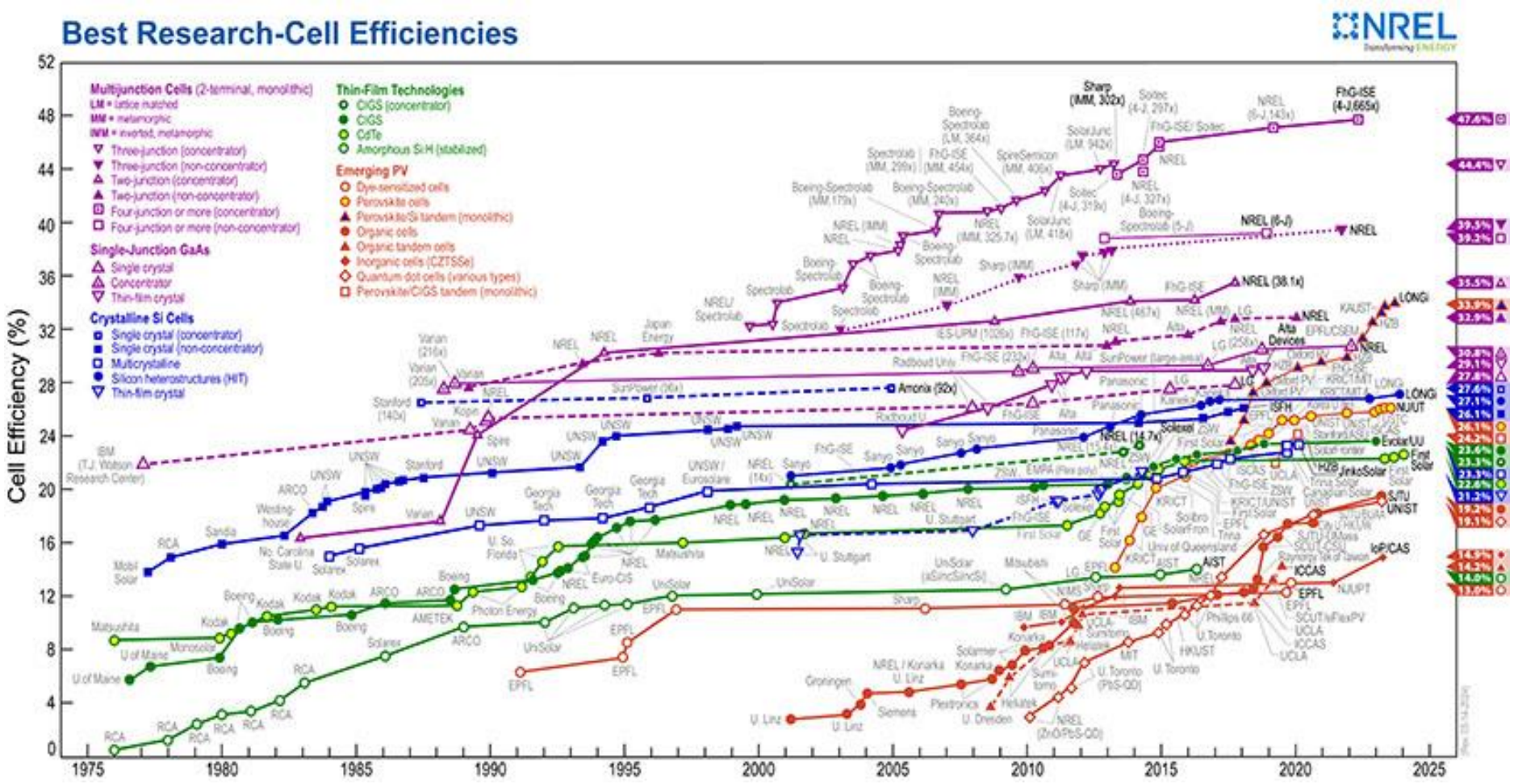

Figure 1-3. The best research solar cell efficiencies from 1976 to 2024.[14]

1-4. Advantages of PSCs

Perovskite solar cells have several key advantages over their competitors.

1) Accessibility of their constituent materials and the ease of depositing the perovskite layer using wet chemistry techniques. [15–21]
2) Direct bandgap – granting a much higher efficiency of light absorption and thus enabling thinner films.[22] These thinner films both reduce material costs and allow flexible solar absorber layers.
3) The bandgap can be tuned by altering the cations or halides (Figure 1-4). This alternation can shift the bandgap between around 1.2 to 3.0 eV.[23] Bandgap tunability enables all perovskite tandem solar cells.[24]
4) Perovskite is an intrinsic semiconductor, reducing recombination issues induced by doping and maximizing charge carrier mobility.[25]

These properties make perovskites a logical first choice for next generation solar cells. However, they have one central issue - stability of both the precursor inks and the resultant devices.

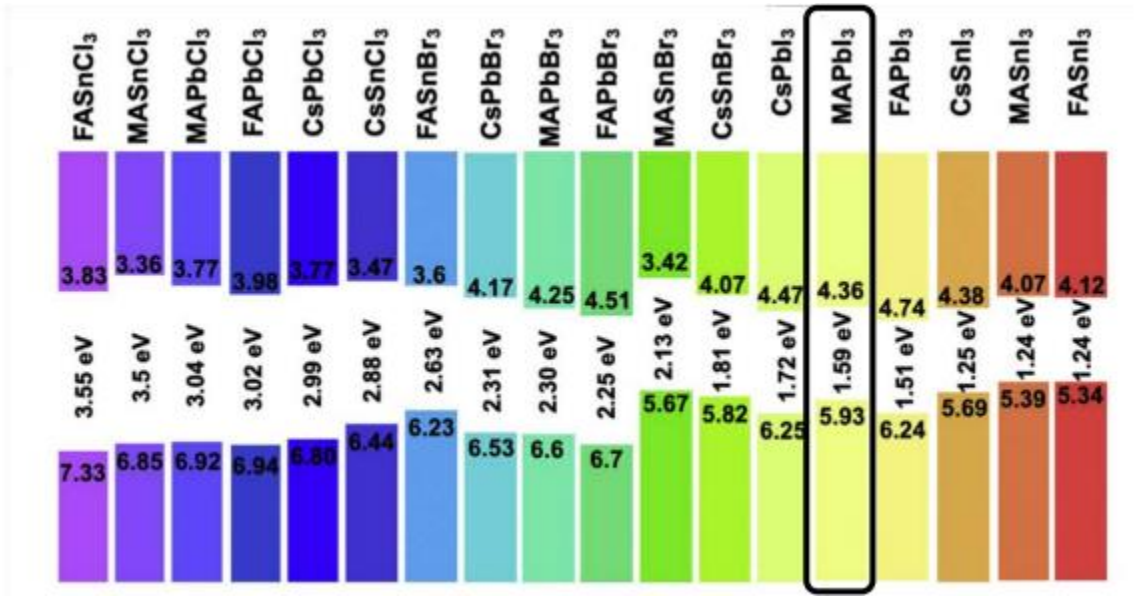

Figure 1-4. Showing various perovskite compositions and the wavelength of their photo luminescence reproduced from [13] an open access article.

1-5. Complications to Perovskite Industrial Scale-up

Current lead halide perovskite devices are highly unstable. This instability takes a variety of forms and presents several challenges, including chemical reactivity, photo instability, thermal instability and, specific to formamidium perovskites, phase stability.

The components of perovskite are reactive under atmospheric conditions. The halides in perovskites react with atmospheric oxygen under UV to form dihalides. Lead halide perovskites undergo hydrolysis when exposed to atmospheric moisture, degrading back into separate lead and organic salts, which then degrade into various other forms based on their halide and organic cation composition. Methylammonium lead halides, the most common light absorber in PSCs, also suffer from the high volatility of the deprotonated form of methylammonium. Encapsulation has so far proven to be the most effective way of alleviating the chemical instability of the devices. This encapsulation layer, either in the form of the top HTL/ETL or an additional layer on top, must be airtight and hydrophobic.[26]

The thermal instability of perovskites arises from the chemical instability of the cation, which can breakdown into their deprotonated form and hydrogen halide even under inert conditions. This is exacerbated by perovskite's low level of thermal conductivity which enables heat to concentrate under operational conditions.[26]

The metal oxide nanoparticles commonly used as ETLs for their excellent electronic and chemical properties have been found to also catalyze the breakdown of perovskites under operating conditions. These properties are their excellent charge carrier mobility, insolvency in perovskite precursor inks, appropriate energy alignment and high transparency. Unfortunately, under operational conditions, namely exposure to UV light, these nanoparticles behave as efficient catalysts for REDOX reactions, including the splitting of the perovskite into their lead halide and organic halide salts, and the subsequent reduction of Pb^{2+} to Pb^{0} with an accompanying buildup of molecular halide. Titanium oxide and tin oxide both serve to produce this effect. There are several solutions, including: the replacement of these excellent ETLS, injection of a

chemically inert layer between ETL and perovskite, the down conversion of UV light via luminescence or filtering it out[27], and the incorporation of sacrificial reductants to slow the process.[28]

Perovskites form different black, optically active, crystal polymorphs: α- (cubic), β- (tetragonal), and γ- (orthorhombic). Though for $FAPbI_3$, these phases are only meta-stable at room temperature; this perovskite converts to optically inactive δ-phase over time. See Figure 1-5 for graphical representations. This issue can be resolved by using various additives to raise the energy barrier for phase transformation.[29]

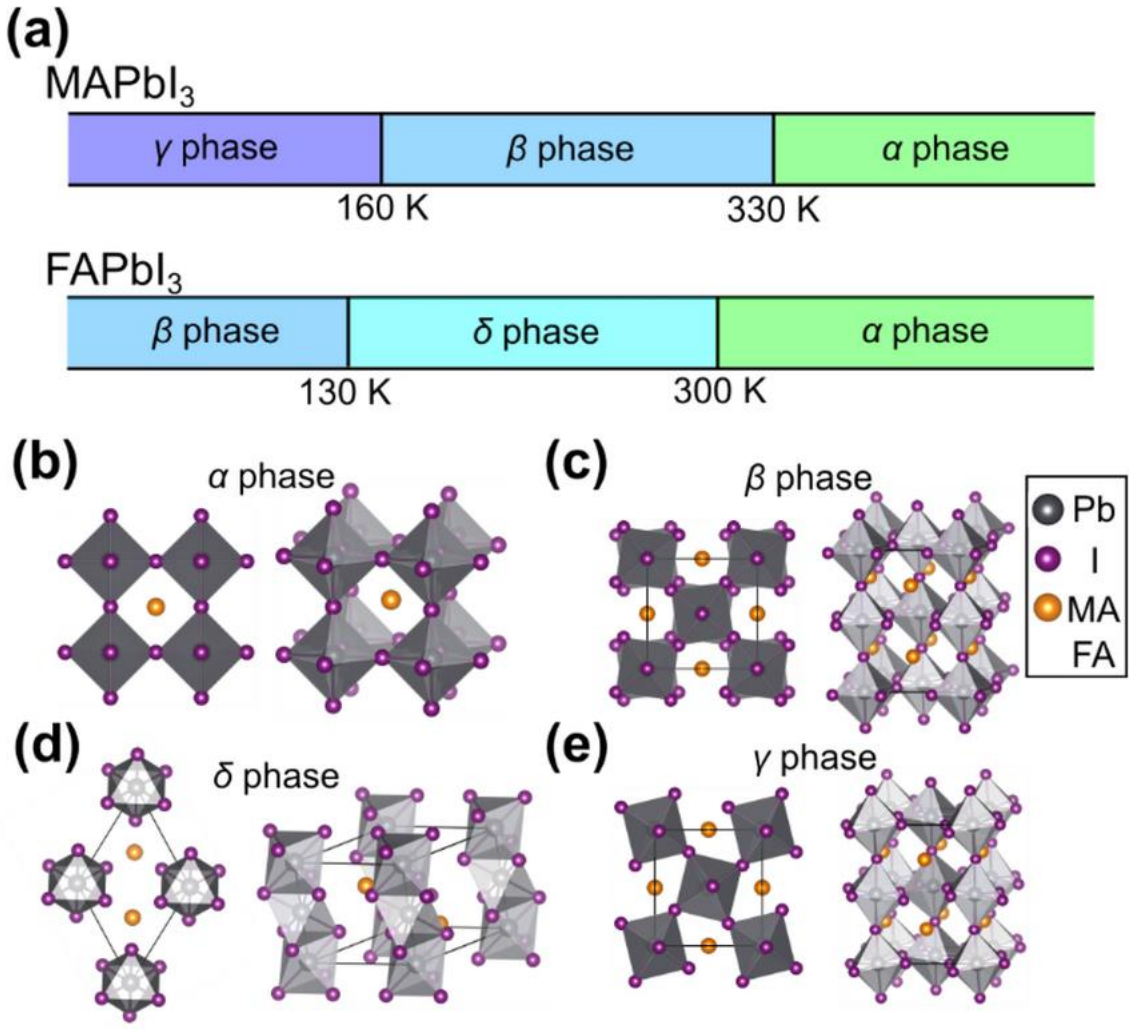

Figure 1-5. (a) The most thermally favored phase for $MAPbI_3$ and $FAPbI_3$ at various temperatures. (b) Cubic alpha (α) phase, (c) the tetragonal beta (β) phase, (d) the trigonal delta (δ) phase, and (e) the orthorhombic gamma (γ) phase. Reproduced from [30] published under open access.

1-6. Ink Instability of Perovskites

The perovskite precursor solution or ink, made by dissolving precursor salts in solvents, can be deposited by a variety of readily available methods and annealed to form a perovskite thin film. However, recent studies showed that the perovskite ink undergoes multiple degradation pathways, as depicted in Figure 1-6, presenting a significant challenge for PSCs to become a competitive commercial option. [31]

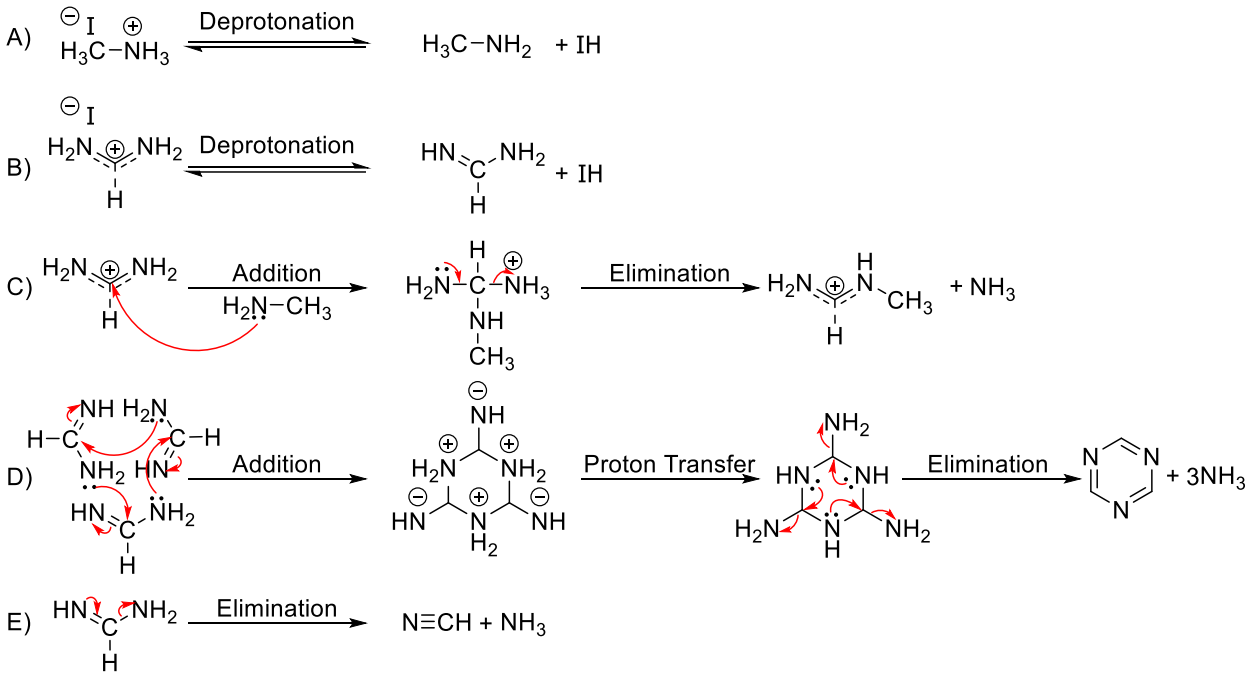

Figure 1-6. Schematic of degradation pathways in perovskite inks: A) Deprotonation of MA^+;[32] B) Deprotonation of FA^+; C) Addition of MA to FA^+ to form MFA^+;[33] D) FA condensation reaction to sym triazine;[34,35] E) FA elimination reaction to form hydrocyanic acid.[35]

A perovskite ink that is suitable for scalable coating of films contains additional components that further exacerbates instability of the ink. For instance, *N*-methyl-2-pyrrolidone (NMP) is typically used as a cosolvent alongside 2-methoxy-ethanol (2ME) in scalable perovskite inks to widen the processing window, and to slow down crystallization, thus resulting in a denser, smoother film with larger grains and more efficient PSCs.[36–39] The NMP operates as a Lewis base to form adducts and complexes with perovskite

precursors enabling homogenous nucleation and inducing the formation of optically active perovskite phase of formamidinium lead iodide (α-$FAPbI_3$).[40–42] However, NMP dramatically accelerates the reactions between the organic cations (reactions depicted in Scheme C and D above).[43] This co-solvent, despite its issues, is needed for scalable coating of perovskite films. Methylammonium chloride (MACl) is another additive widely used in perovskite inks to lower the energy barrier for the transition to α-$FAPbI_3$ and improve crystal density.[44–46] However, the MA^+ cation deprotonates to MA, which then reacts with the FA^+ in solution to form methyl formamidinium (MFA^+)[47] (Schemes A and C in Figure 1.6). This reaction not only removes FA from the solution but also competitively forms optically inactive $MFAPbI_3$.[43,48]

Multiple stabilizers have been reported to prevent some degradation pathways in perovskite inks. Sulfur, for instance, was found to prevent the deprotonation that initiates the FA^+ and MA^+ to MFA^+ and $DMFA^+$ reactions, as well as the FA^+ self reaction to form sym-triazine and cyanide (Figure1-6 A to E).[43,49,50] Unfortunately, sulfur is not a suitable stabilizer for the perovskite ink optimized for scalable fabrication of films due to its insolubility in the primary solvent, 2ME. This solvent cannot be swapped out as it can form a uniform and conformal precursor film due to its rapid evaporation.[51,52] Reactions in Figure 1-6 C to E require the deprotonated form of either MA^+ (MA) or FA^+ (FA) to proceed[35,53–55]; thus, protonation of the solution is another viable strategy to stop all three forms of FA loss.[56,57] Addition of organic acids has been found to be a viable method of minimizing this,[56,58,59] as has addition of easily deprotonated alkanes.[60] Hydroiodic acid is another stabilizer previously studied to protonate the ink, but it has also been found unsuitable due to its water content and the fact that it is a strong acid.[34]

An ideal stabilizer of perovskite ink should prevent all known degradation pathways shown in Figure 1.6. In other words, an ideal stabilizer should be: 1) a weak Brønsted-Lowry acid to protonate the solution without solvent reactions[61], eventually preventing loss of organic cations; 2) a mild reducing agent to prevent loss of iodide; 3) readily soluble in polar solvents; and, 4) ideally be a solid to not alter the perovskite ink solvent matrix. These same criteria are often used in biochemistry research, which is typically done in polar solvents, to simulate in vivo conditions. Benzylhydrazine, for instance, is often used

in biochemistry to reduce enzymes in an acidic medium[62]; benzylhydrazine hydrochloride (BHC) was indeed recently reported to be a promising perovskite precursor stabilizer to act as a sacrificial reductant in solution and in films to prevent I_2 buildup.[28,59] Another reason that benzylhydrazine is used for in biochemistry is to prevent oxidative deamination, a process that bears certain similarities to the mechanism of FA breakdown shown in Figure 1-6.[62] However, whether BHC can prevent FA breakdown pathways in perovskite inks is yet to be studied. It also remains to be known what BHC converts to in perovskite inks, and how these products would affect the quality of perovskite films and performance of ultimate solar cells.

This thesis uncovers multiple additional stabilization effects of BHC in perovskite inks. We show that it protonates the solution as a weak organic acid; it also reacts with the trace water in the solvent to reduce water assisted deprotonation; and, when it fully reacts, BHC's ultimate form is chemically benign and does not worsen perovskite crystallization or its device performance.

Chapter 2. Methodology

2-1. Abstract

In order to characterize both the impact of benzylhydrazine hydrochloride (BHC) on ink stability and BHC's own lifetime transformations, a series of experiments were carried out. The impact of BHC was first used as an additive in ink and compared with an identically prepared control ink in order to verify the extent of its stabilizing effects via NMR of the inks and XRD on the resultant thin films over time. Then BHC and iodine were studied in isolation, in order to understand the cause of the stabilization effects as well as to uncover the final products. Finally, films and devices were made with BHC and control inks to verify that this additional stabilization was not at the cost of film quality or device efficiency.

2-2. Materials and Solution Preparation

ITO coated glass substrates were purchased from Shang Yang Solar (X07-10 A). Tin (IV) oxide (SnO_2) 15% in H_2O colloidal dispersion solution was purchased from Alfa Aesar. The formadimidium iodide ($CH(NH_2)_2I$, 99.99%), and methylammonium chloride (CH_3NH_3Cl) were purchased from Greatcell Solar. Lead iodide (PbI_2, 99%) was purchased from TCI Chemicals. 1-Methyl-2-pyrrolidinone, cobalt salt (FK 209 Co(III) TFSI), 4-tert-Butylpyridine (tBP, 98%), and bis (trifluoromethane) sulfonimide lithium salt (Li-TFSI 99.95%) were purchased from Millipore Sigma. Sprio-OMeTAD was purchased from Xi'an Polymer Light Technology Co., Ltd.

Preparation of Spiro-OMeTAD solution

Spiro-OMeTAD (0.1 g) was dissolved in chlorobenzene (1.1 mL). Additionally, 23 μL of Li-TFSI solution (520 mg mL^{-1} in acetonitrile), 39 μL of tBP and 10 μL of FK 209 Co(III) TFSI solution (375 mg mL^{-1} in acetonitrile) was mixed in the Spiro solution and filtered before use.

Preparation of SnO_2 solution

SnO_2 solution was made up of H_2O:IPA:SnO_2 15% colloid suspension at a 3:3:1 volumetric ratio, respectively.

Preparation of Precursor Inks

1M perovskite precursor solutions were prepared by dissolving 1M FAI and 1M PbI2 in 2-methoxyethanol and *N*-Methyl-2-pyrrolidone at a 0.95/0.05 solvent ratio along with 0.3M MACl and 0.25μM L-α-Phosphatidylcholine to improve film quality. 1.2 mM of BHC was added to the non-control solution. All precursor solutions were stored in glass vials with PTFE-lined plastic caps within a laboratory fumehood and were only opened as necessary for analysis.

2-3. Characterization

Photovoltaic parameters were determined employing a Newport Oriel sol-3 A (class AAA) solar simulator at the standard AM 1.5 solar irradiance. Data acquisition occurred through an Ossila source meter, scanning the cell voltage from 1.2 to -0.100 V (Figure 2-1).

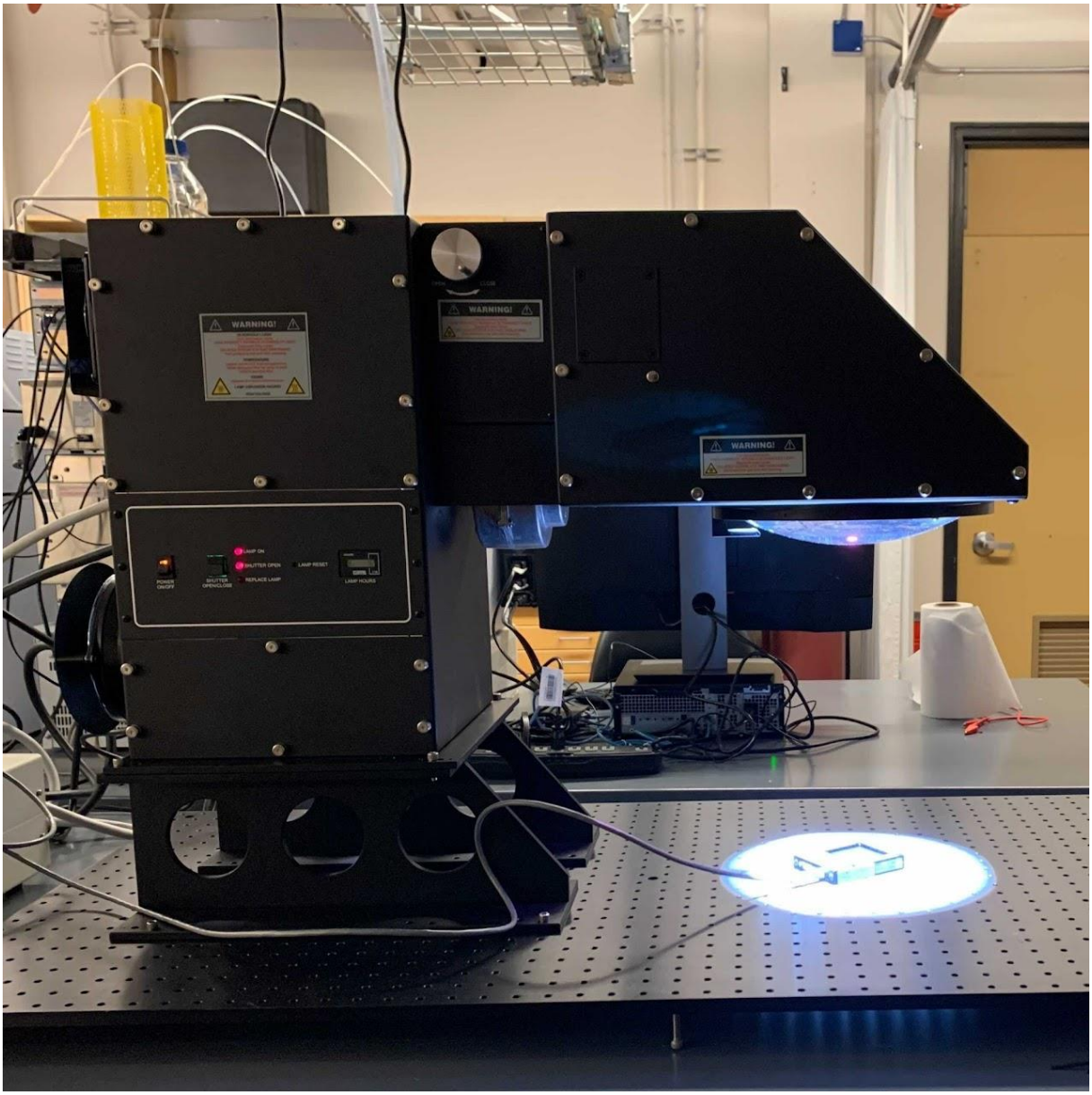

Figure 2-1. Solar simulator and device holder.

XRD measurements were done with a PANalytical Empyrean system using a Cu (Kα, 1.5406 Å) source. SEM images were obtained with a Hitachi S-4800 field emission SEM.

BHC NMR spectra were acquired using a 0.2M BHC and 0.25M iodine sample in pure deuterated DMSO. This solution was left to react for 6 hours, before an initial ^{1}H NMR was acquired, then a 16-hour long NMR experiment was run on it, acquiring ^{1}H-^{13}C, Heteronuclear Single Quantum Coherence (HSQC),

and ^{1}H-^{15}N, ^{1}H-^{13}C Heteronuclear Multiple Bond Correlation (HMBC) spectra. Finally, an additional ^{1}H NMR run was done to identify the terminal product. Aforementioned spectra were acquired with a Bruker AVANCE-I Neo 500 MHz spectrometer. The ink spectra were acquired with a Bruker AVANCE-III Neo 300 MHz spectrometer.

Photoluminescence spectra were captured using a Renishaw inVia Raman Microscope equipped with a 632.8 nm (He–Ne) excitation laser.

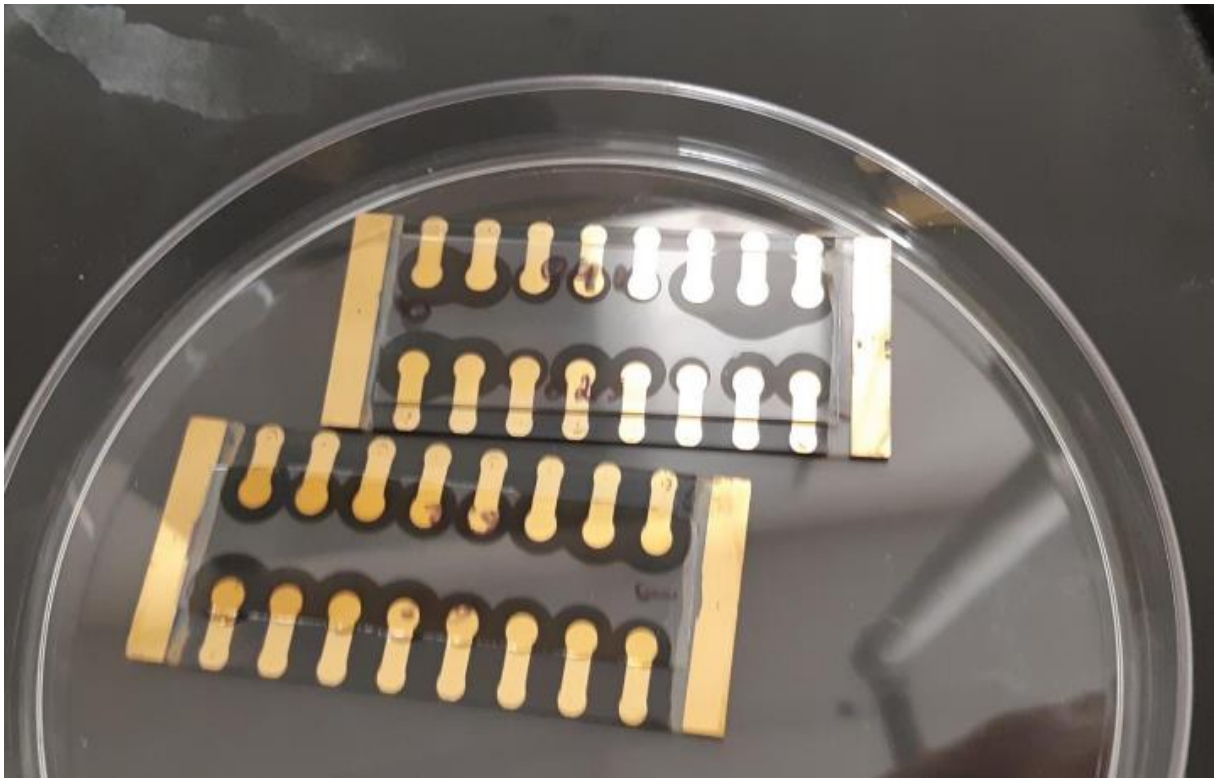

Figure 2-2. Image of fully fabricated devices.

2-4. Device Fabrication

Patterned 3.25 × 7.5 cm glass/ITO substrates were cleaned successively with deionized water, acetone, and IPA by sonication for 15 min each and dried them in oven. The cleaned substrates were then ozone treated for 15 min. 30 μL of SnO_2 solution was deposited three times by blade coater (Figure 2-3), (ZEHNTNER ZAA 2300 automatic film applicator) on a base heated to 71°C at a rate of 10 mm/s and a

blade height of 855 µm and then annealed at 150°C for 30 minutes. 28 µL of Perovskite solution was deposited once by blade coater at a rate of 10 mm/s with a gap height of 900 µm with a N_2 air knife blowing at a pressure of 25 psi, this was then annealed at 130°C for 1 minute followed by 150°C for 30 minutes. 35 µL of spiro solution was deposited by blade coater on a base heated to 48.9 °C at a rate of 30 mm/s with a gap height of 850 µm and not annealed.

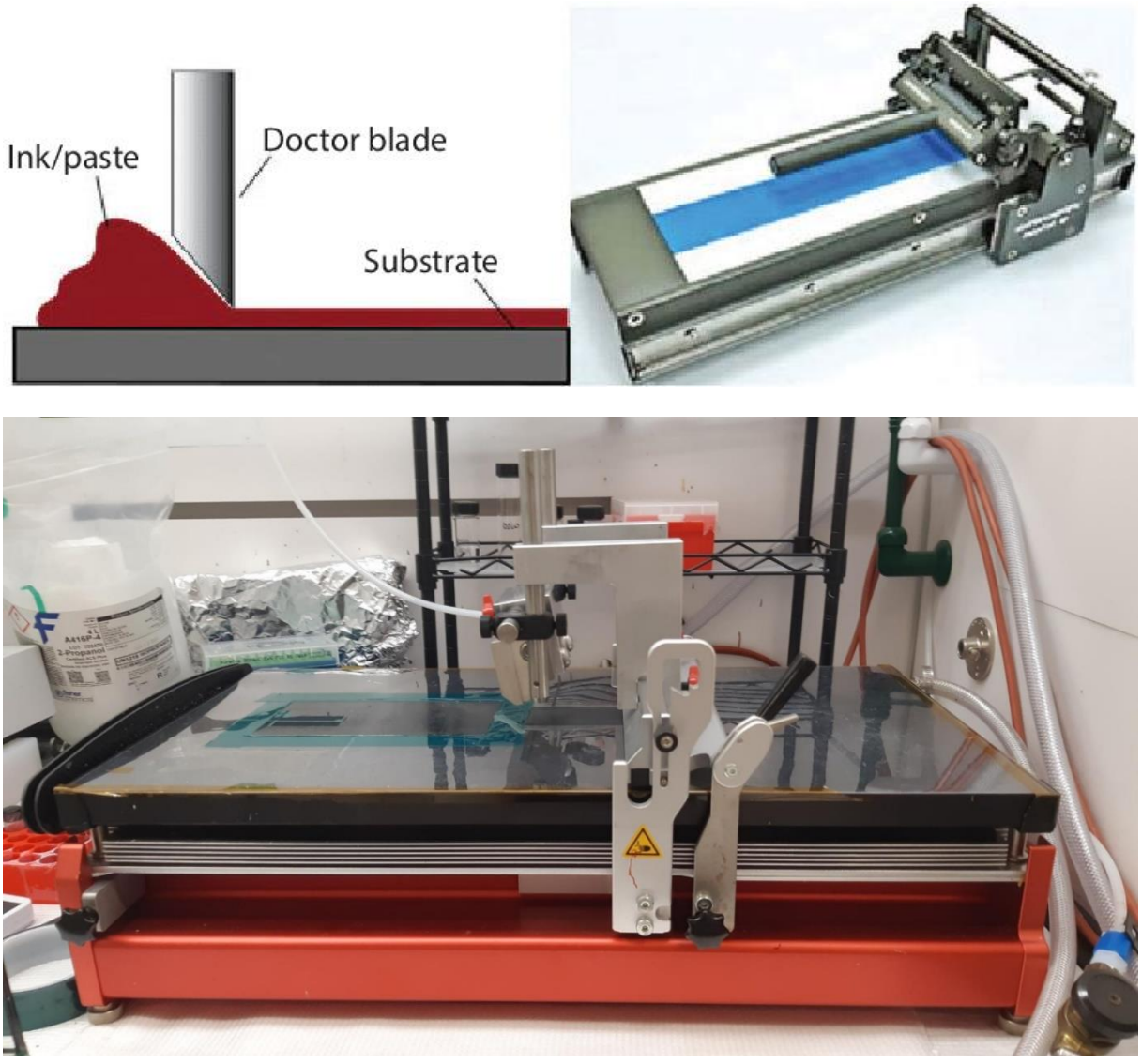

Figure 2-3. Diagram of blade coater function reproduced with permission from [63] copyright (2017) and image of blade coater used.

Finally, gold electrodes with a thickness of 80 nm and an active area of 0.049cm^2 were applied using EvoVac thermal evaporation system by Angstrom Engineering Inc., under a vacuum of 10^{-6} Torr (Figure 2-4).

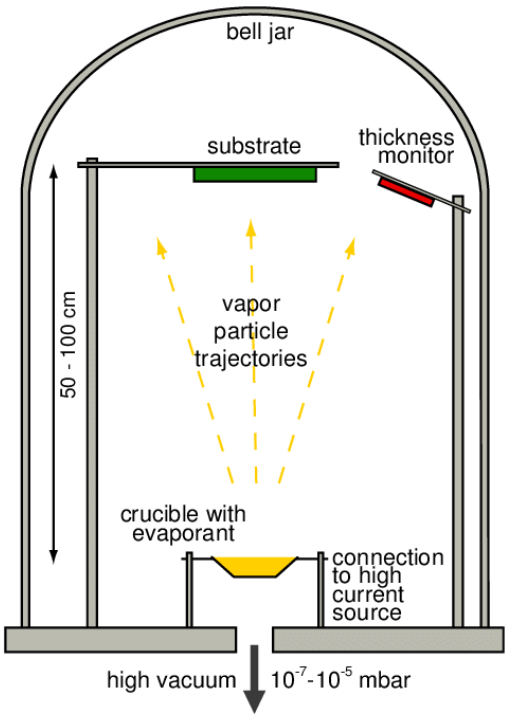

Figure 2-4. Diagram of thermal evaporator reproduced from [64] an open access article.

Chapter 3. Results and Analysis

Note: This chapter is based on my first-authored paper submitted to a journal. The paper has multi-author contributors. I have contributed to planning experiments, performing the ink NMR and XRD experiments, as well as the bulk of the analysis, writing, and editing.

3-1. Abstract

Perovskite precursor inks suffer various forms of degradation, such as iodide anion oxidation and organic cation breakdown, hindering reliable perovskite solar cell manufacturing. Here we report that benzylhydrazine hydrochloride (BHC) not only retards the buildup of iodine as previously reported but also prevents the breakdown of organic cations. Through investigating BHC and iodine chemical reactions, we elucidate protonation and dehydration mechanisms, converting BHC to harmless volatile compounds, thus preserving perovskite film crystallization and solar cell performance. This inhibition effect lasts nearly a month with minimal BHC, in contrast to control inks where organic cations fully react in less than a week. This enhanced understanding, from additive stabilization to end products, promises improved perovskite solar cell production reliability.

3-2. NMR analysis of aging ink

We used ^{1}H NMR to track degradation pathways of organic components of the ink. The precise tracking of FA breakdown is difficult due to it forming several products (Figure 1-6 C to E) and the overlap of their ^{1}H NMR peaks (Figure 3-1 A): the peak corresponding to sym-triazine (Figure 1-6 D) occurs at 9.3 ppm which overlaps with the central amine proton of MFA (Figure 1-6 C), making it difficult to directly quantify them; the hydrocyanic acid (Figure 1-6 E) has a very low boiling point (25.6°C) and a high volatility, meaning it is easily lost to vaporization. Regardless of chemical pathway, for each mole of FA lost one mole of ammonia is produced. Hence, we instead focused on tracking ammonia which is equimolar to the lost FA. The ammonia was protonated to ammonium via the addition of a small amount of hydroiodic

acid (1 µL into 600 µL ink aliquots) which then appears as a distinct 1:1:1 triplet at 7.08 ppm in the ^{1}H NMR spectrum.[65]

Figures 3-1 B and C show relative molarities of remaining and lost FA^{+} (equimolar to NH_4^{+}) in the inks, with and without BHC, after aging. Nearly half of FA^{+} was lost in the control ink within 5 days of aging, while we observed only 3% FA^{+} loss in the presence of BHC during that same time. NMR figures also show that the loss of FA^{+} slows massively once the MA^{+} has been completely used up, as the reaction of MA^{0} with FA^{+} to form MFA^{+} (Figure 1-6 C) is the dominant FA degradation pathway.[43,47] Therefore, the control ink has a much-retarded FA^{+} loss rate following the complete loss of MA^{+} after 5 days of aging.

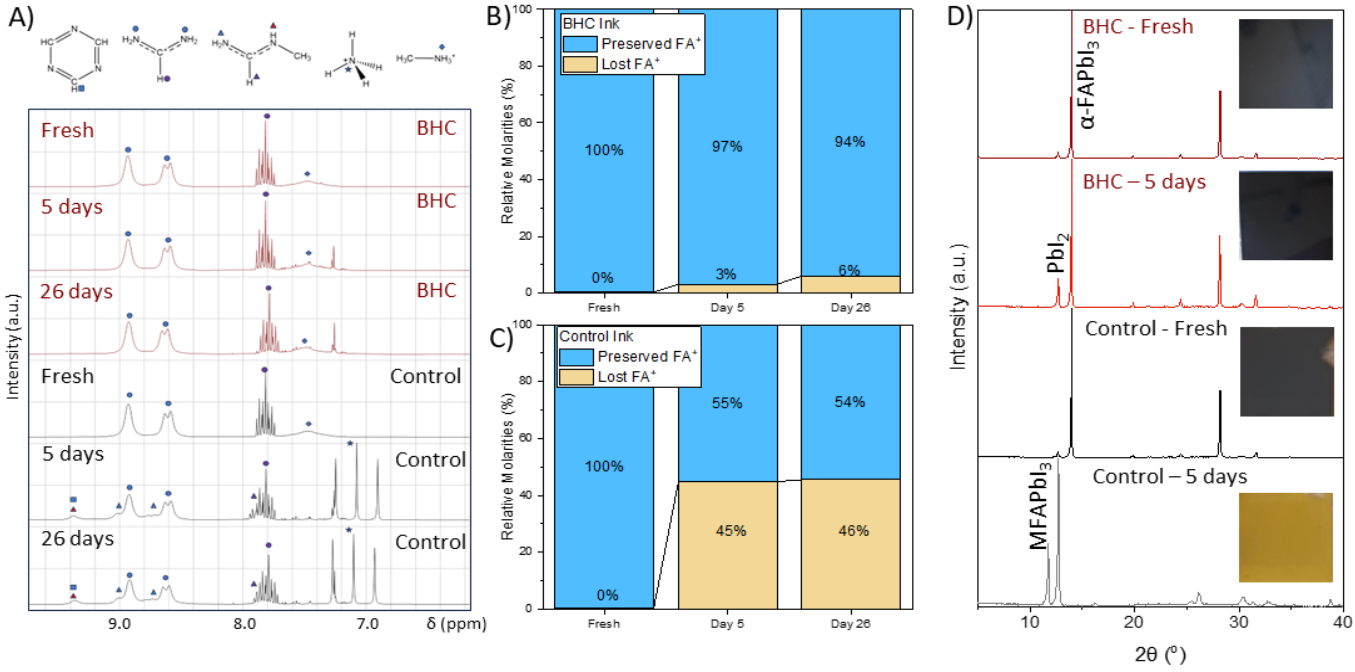

Figure 3-1. Characterization of perovskite ink with and without BHC after aging: A) ^{1}H NMR spectra of perovskite solutions over time along with peak assignments for FA^{+} and its degradation products. Red-colored spectra represent BHC-doped ink, the black-colored spectra represent the control ink. B and C) Integration values of ^{1}H NMR peaks originating from FA in control and BHC-inks. D) XRD profiles of

films made with fresh ink and 5-day old ink. Insets are the images of corresponding films. Note the overlap of the fresh and day 5 ink XRD results for the BHC doped ink.

We have also performed visual and structural inspection of the films prepared from fresh and aged inks. Both BHC doped and control inks, when fresh, turned black upon annealing (Figure 3-1 D), indicating formation of the α-phase perovskite. This was further confirmed by the XRD results.

After five days of aging of inks, the BHC-doped ink formed a black film which was visually and structurally identical with the film made by fresh ink (Figure 3-1 D). However, the film created by the 5-day aged control ink was yellow, which would normally indicate δ-phase perovskite (Figure 3-1 D). Additionally, there is a strong diffraction peak in the control ink at $2\theta=11.7^{o}$, very close to the expected δ-phase (2H) peak at 11.8^{o}. However, the yellow film failed to form a black α-phase perovskite when heated to 150°C indicating that it is instead a non-perovskite phase formed from organic degradation products, principally MFA^{+} (the δ-phase would convert to black alpha-phase at 150°C).[43]

We then attempted to restore the aged control ink by adding the BHC. This changed the colour of the ink from orange back to yellow, indicating a reduction of the iodine species but the ink still failed to produce a black α-phase of perovskite film. Further, BHC addition up to 0.1M (~100× more than in the BHC-doped ink) also failed to make the ink viable (Figure 3-2) and resulted in yellowish films. Thus, the failure of the ink cannot be attributed to the reversible iodide to iodine reaction as the addition of excess reductant could not restore the ink. We hence conclude that BHC has additional benefits to ink stability besides reducing iodine, as we will reveal below.

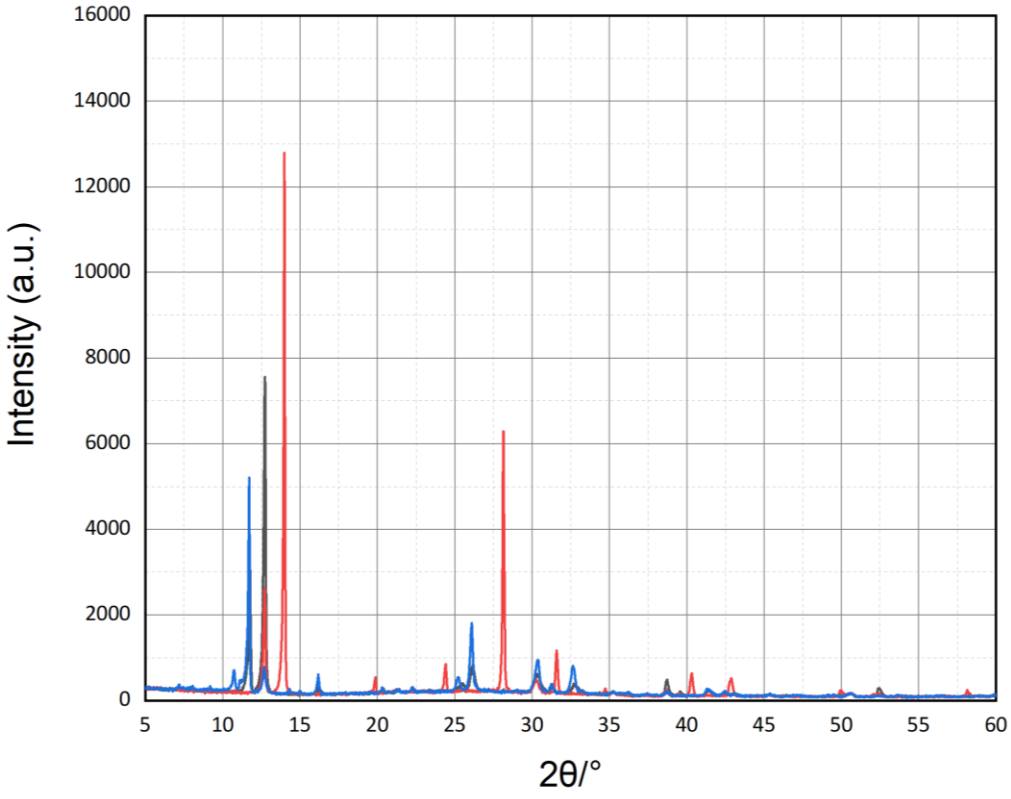

Figure 3-2. XRD of films made with 5-day-old ink. Red trace is BHC doped film; black trace is control film; blue trace is control ink with 1mg/mL BHC.

3-3. Full lifetime analysis of benzyhydrazine

To understand the full impact of BHC on the ink, a detailed NMR study; ^{1}H, ^{1}H-^{13}C, Heteronuclear Single Quantum Coherence (HSQC), and ^{1}H-^{15}N, ^{1}H-^{13}C Heteronuclear Multiple Bond Correlation (HMBC) was performed on the reaction of BHC and iodine in isolation. The ^{1}H, ^{1}H-^{13}C, HSQCs and ^{1}H-^{15}N HMBC were used to identify functional groups and bridging methylene carbon/hydrogen pairs. Then, HMBC was used to verify that these structures were bonded to the phenyl ring. A solution of BHC and a small excess of iodine was made up in dimethyl sulfoxide-d_6. This solution was left to react for 6 hours before the NMR studies. An additional ^{1}H NMR scan was performed at the end of the 16-hour long sequence.

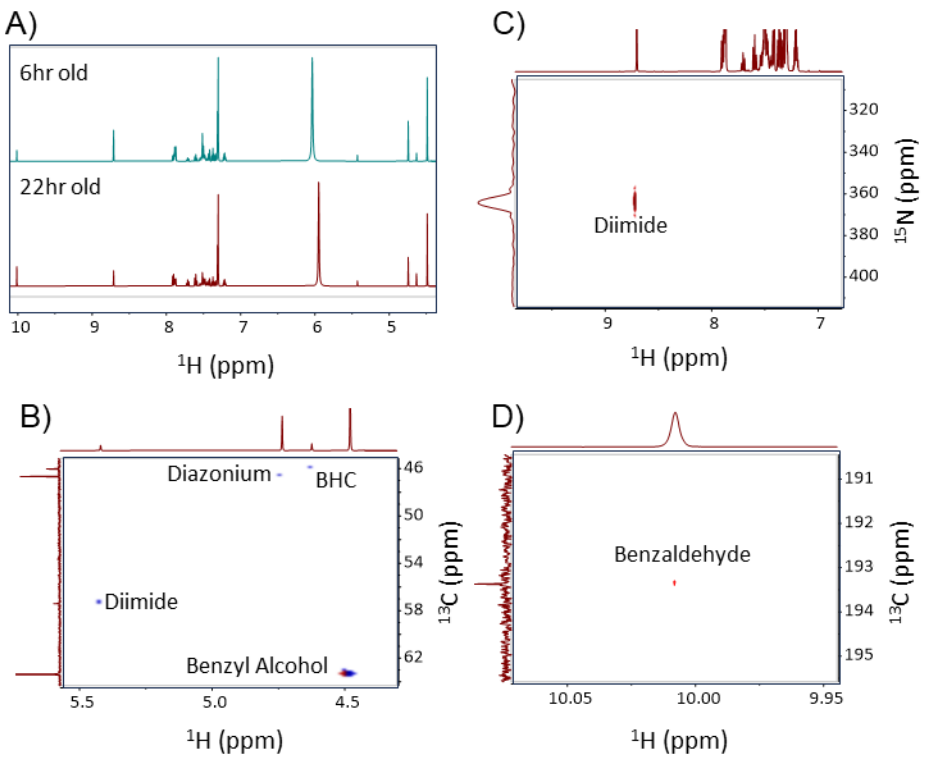

Figure 3-3. Full lifetime analysis of benzylhydrazine: A) ^{1}H NMR of BHC and its oxidation products after being allowed to react for 6 and 22 hrs at the beginning and end of the 16-hour NMR run. B) ^{1}H-^{13}C HSQC focused on bridging -CH_2- section. C) ^{1}H-^{15}N HSQC D) ^{1}H-^{13}C HSQC focused on aldehyde section.

The (^{1}H,^{13}C) (10.1 δ,193.4 δ) peak shown in Figure 3-3 D represents a typical aldehyde signature. From the increasing value of the ^{1}H signal peak at δ=10.1 over 16 hours seen in Figure 3-3 A, the aldehyde is identified as the final product. The presence of this aldehyde is confirmed by HSQC of isolated benzaldehyde (Figure 3-4 A). This agrees with previous work in the biochemistry and organic chemistry fields that have shown that benzylic diazonium converts to benzyl alcohol and can then be oxidized to benzaldehyde under aqueous conditions.[62,66–68] The extremely downfield ^{1}H-^{15}N HSQC shown in Figure 2 C is identified as a diimide or azo compound. Four bridging Ph-CH_2-X HSQC signals are identified between 4.5 and 5.5 (Figure 3-3 B). The relevant functional groups are assigned as follows: (^{1}H: δ 4.48, ^{13}C: δ 63.4) benzyl alcohol; (^{1}H: δ 4.64, ^{13}C: 45.96) BHC; (^{1}H: δ 4.74, ^{13}C: 46.63) diazonium; and (^{1}H: δ 5.43, ^{13}C: 57.42) a diimide. The benzyl diazonium is likely stabilized by the use of DMSO as a solvent, enabling its

detection.[68] The presence of alcohol was further confirmed by comparison with an authentic standard (Figure 3-4 B).

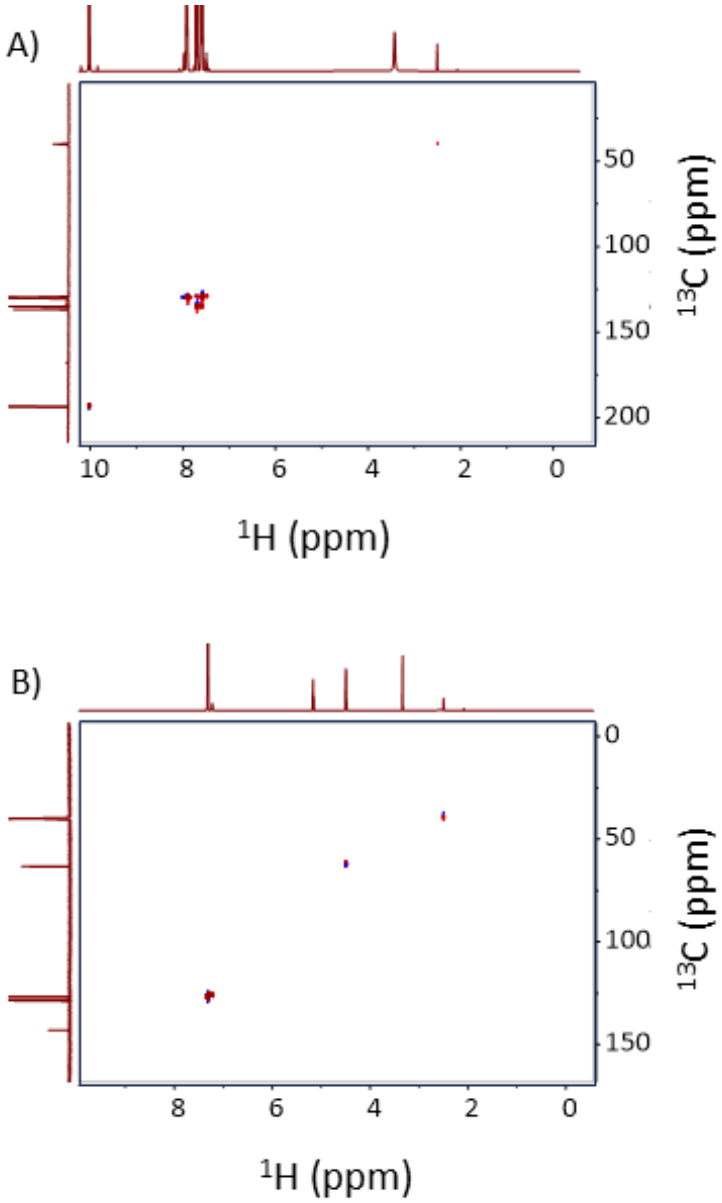

Figure 3-4. A) Benzaldehyde HSQC; B) Benzylalcohol HSQC.

The above assignments were made by comparing to experimental and literature values. Based on these intermediates, and the final product, we proposed the following reaction scheme to represent the full lifetime cycle of BHC:

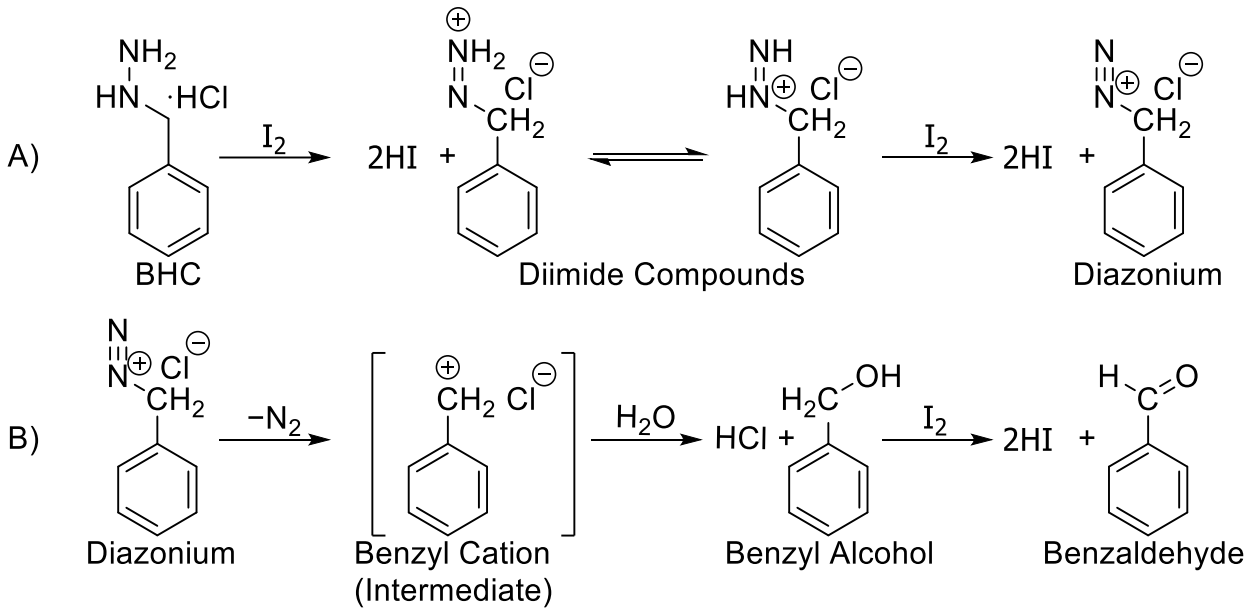

Figure 3-5. BHC conversion pathway schemes in a solvent that resembles perovskite ink: A) Reaction of BHC and iodine to form a diazonium salt. B) Substitution of nitrogen leaving group with hydroxyl group and subsequent oxidation to aldehyde.

The reaction schemes in Figure 3-5 reveal the source of the improved chemical stability of target perovskite ink, with each mole of BHC releasing seven moles of free protons and absorbing one mole of water. Protonation of the perovskite precursor solution can prevent Figure 1-6 A and B reactions, which in turn prevents Figure 1-6 C to E reactions. Additionally, small quantities of water which typically exist in the original solvent mixture is known to greatly accelerate the loss of organic cations by facilitating their deprotonation.[43,57] The conversion of the diazonium ion to a benzyl alcohol consumes water (Figure 3-5 B). This removal of water by BHC is further evidenced by the lack of a distinct 3.3 δ ^{1}H NMR peak (Figure 3-6) typical of the unavoidable water contamination of DMSO d_6[69]. The final conversion to benzaldehyde proceeds by a typical dihalide oxidation/elimination mechanism with the alcohol engaging in a nucleophilic attack on the dihalide generating an OX intermediate followed by deprotonation of the carbon by DMSO

acting as a weak base. This same reaction sequence also appears to apply to the free base of the BHC salt (Figure 3-7).

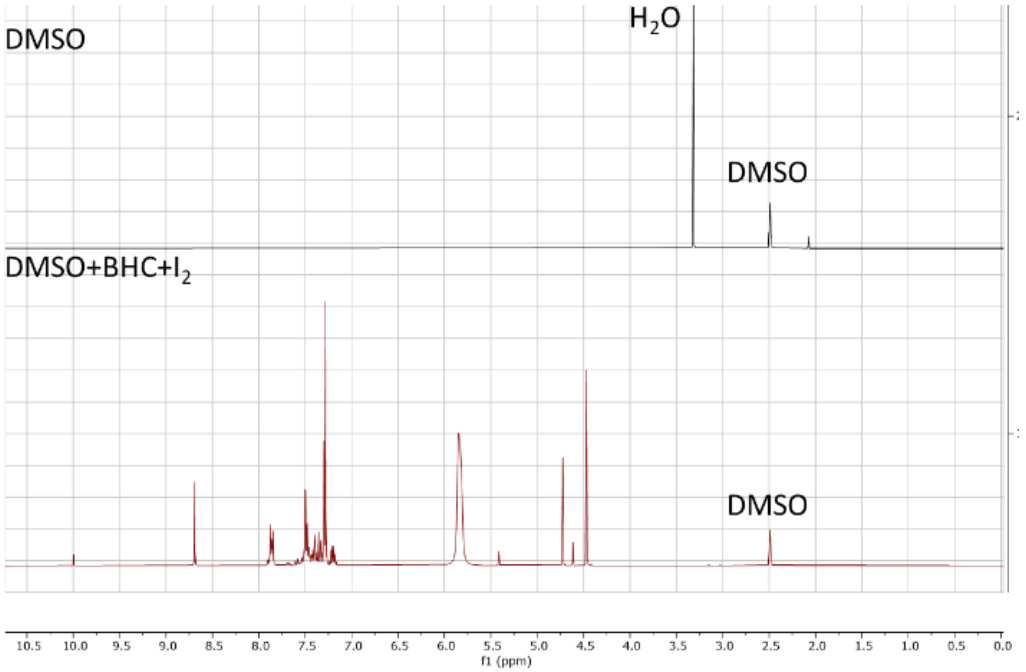

Figure 3-6. DMSO d_6 before and after the addition of 0.2M of BHC and 0.25M of I_2. Note the significant H_2O peak at 3.31 δ in the ^1H NMR.

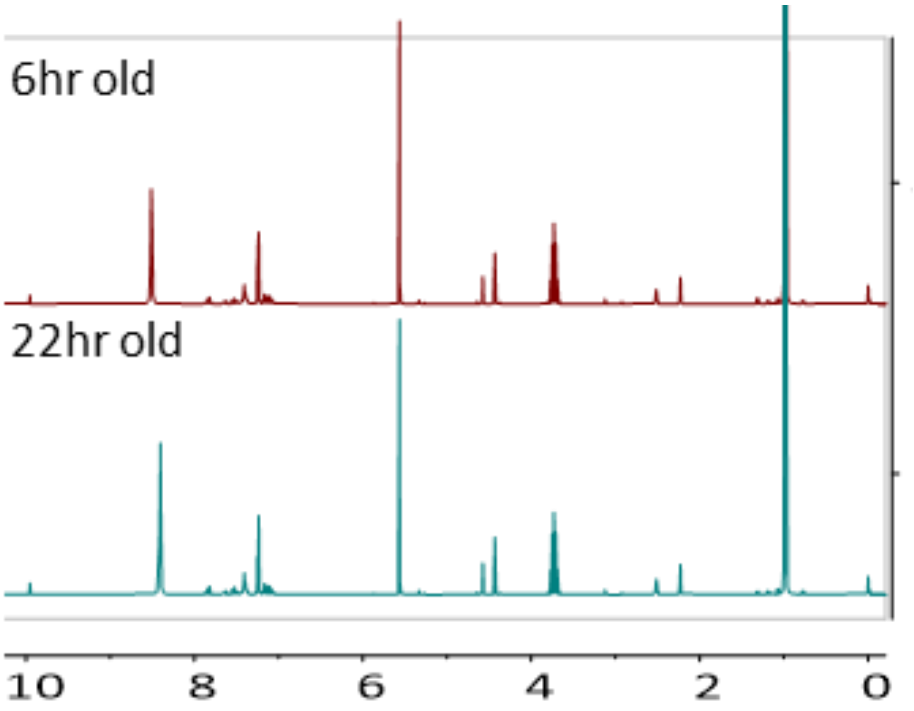

Figure 3-7. ^{1}H NMR of freebase BHC and its oxidation after 6-hours of reaction time and 22-hours of reaction time.

3-4. The impact of BHC on the performance of perovskite solar cells

To verify that the increased ink stability was not at a cost of efficiency of ultimate devices, we fabricated perovskite solar cells in an indium tin oxide (ITO)/SnO_2/perovskite/spiro-OMeTAD/gold (Au) structure. All layers listed were blade coated in ambient air, except for the deposition of the gold electrode which was prepared by thermal evaporation. The BHC devices performed better both on average and in terms of the champion device, achieving an efficiency of 19.6% (Figure 3-8 C). This device had a fill factor (FF) of 76.9%, a short-circuit current (J_{sc}) of 25.1 mA cm^{-2} and an open-circuit voltage (V_{oc}) of 1.02 V (Figure 3-8 D). The champion control device had a PCE of 19.1%, a FF of 78.6%, a J_{sc} of 24.9 mAcm^{-2} and a V_{oc} 0.975V. Figure 3-9 provides further device statistics.

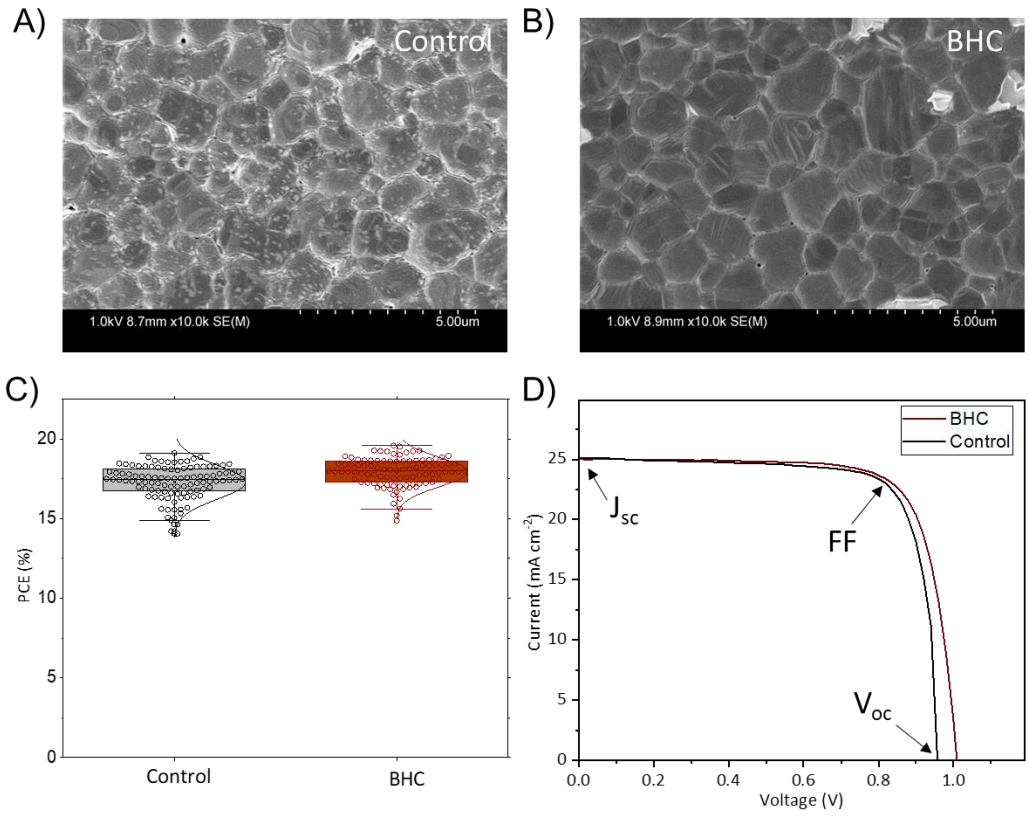

Figure 3-8. Characterization of films and devices. A-B) Surface SEM images of films made from fresh control and BHC-doped inks. C) Efficiency of 104 control and 95 BHC-doped perovskite solar cells. The boxes indicate the 25th and 75th percentiles. The whiskers indicate the 5th and 95th percentiles. The mean is represented by the line dividing the boxes. D) J-V curve of champion pixel from both devices.

To further confirm the quality of perovskite films, we studied their morphology with a scanning electron microscope (SEM). Figures 3-8 A and B show compact films without pinholes. Bright particulates seen in Figure 3-8 A are due to lead iodide (as organic cations are lost in the control ink, stoichiometric control is lost and free lead iodide is found in the resultant film), a lack of stoichiometric ratio management in the control ink might explain the lower reproducibility of the resultant devices. [70,71]

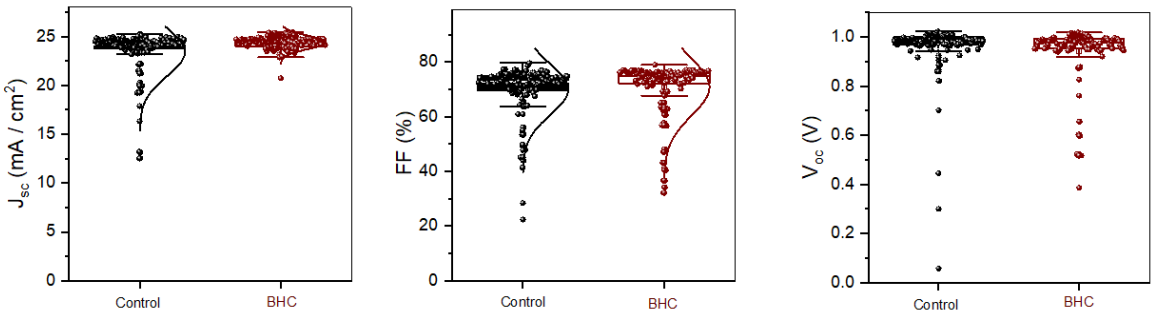

Figure 3-9. Statistic data of photovoltaic parameters: J_{SC}, fill factor and V_{OC} from left to right for devices made with control and BHC doped ink. The boxes indicate the 25th and 75th percentiles. The whiskers indicate the 5th and 95th percentiles. The mean is represented by the line dividing the boxes.

Chapter 4. Conclusions and Outlook

Perovskite solar cells have recently caught up to silicon devices in terms of peak efficiency.[14] As of yet, this is only possible under laboratory conditions and with small area devices. Upscaling techniques that function well in ambient air are being developed at an impressive speed, but there are still instability issues with both the devices and their precursor inks.

The high instability of perovskite precursor inks has proven a significant roadblock to their commercial viability. Borrowing knowledge from the field of biochemistry in preventing amine degradation, we have shown that BHC has additional positive effects on the stability of perovskite ink besides reduction of iodine back to iodide. The cause of this is elucidated by detailed NMR investigation of the products and intermediates, and the reactions that occur to form these compounds. BHC protonates the precursor solution and shifts the equilibrium of the deprotonation reaction of the organic cations back towards the reactants. This deprotonation is the first stage of the various chemical degradation reactions in perovskite ink. BHC also aids stability by absorbing water, due to the electrophilic nature of the resulting diazonium cation. This compound is finally converted to benzaldehyde with some possibly being converted to benzoic acid. Regardless, both these compounds are benign in regard to our ink and can be removed during annealing. We reported nearly 20% efficiency for all-scalable n–i–p $FAPbI_3$ perovskite solar cells using this ink, indicating no loss of efficiency in the presence of BHC.

At present, numerous additives are being used to stabilize both PSCs and the precursor inks. However, they are often understudied in terms of their full chemical impact and lifecycle. More cooperation between engineers and chemists will serve to improve both the studying of, and the communication, around perovskite degradation. There are numerous simultaneous sub-issues to be resolved in order to stabilize

perovskites enough for commercial viability and, without a complete understanding of additive impact, the risk of fixing issues while creating new ones arises. For instance, MACl aids in the stabilization of the optically active α-phase of FAPbI but reacts with FA. These issues are further exacerbated by the tendency in the perovskite field to use a multi-additive stabilization approach, considering each issue and corresponding solution in isolation, then applying all the solutions together without consideration of their potential interactions. This is a place of immense opportunity for interdisciplinary work between material scientists, chemists and engineers. Working together, these disciplines can find new approaches to balance competing demands and create the best possible devices, which will hopefully clear the way to widespread commercialization.

References

(1) Mitzi, D. B. Introduction: Perovskites. *Chem. Rev.* **2019**, *119* (5), 3033–3035. https://doi.org/10.1021/acs.chemrev.8b00800.

(2) Hamukwaya, S. L.; Hao, H.; Zhao, Z.; Dong, J.; Zhong, T.; Xing, J.; Hao, L.; Mashingaidze, M. M. A Review of Recent Developments in Preparation Methods for Large-Area Perovskite Solar Cells. *Coatings* **2022**, *12* (2). https://doi.org/10.3390/coatings12020252.

(3) Li, Y.; Yu, S.; Yang, J.; Zhang, K.; Hu, M.; Qiu, W.; Guo, F.; Qian, W.; Reinecke, S.; Chen, T.; Saidaminov, M. I.; Wang, J.; Yang, S. Filterless Narrowband Photodetectors Enabled by Controllable Band Modulation through Ion Migration: The Case of Halide Perovskites. *InfoMat.* **2024**, *6* (1), e12506. https://doi.org/https://doi.org/10.1002/inf2.12506.

(4) Zhang, D.; Li, D.; Hu, Y.; Mei, A.; Han, H. Degradation Pathways in Perovskite Solar Cells and How to Meet International Standards. *Commun. Mater.* **2022**, *3* (1), 58. https://doi.org/10.1038/s43246-022-00281-z.

(5) Ortega-San-Martin, L. Introduction to Perovskites: A Historical Perspective. In *Revolution of Perovskite: Synthesis, Properties and Applications*; Arul, N. S., Nithya, V. D., Eds.; Springer Singapore: Singapore, 2020; pp 1–41. https://doi.org/10.1007/978-981-15-1267-4_1.

(6) Kim, H.-S.; Im, S. H.; Park, N.-G. Organolead Halide Perovskite: New Horizons in Solar Cell Research. *The Journal of Physical Chemistry C.* **2014**, *118* (11), 5615–5625. https://doi.org/10.1021/jp409025w.

(7) Walsh, J. Ab Initio Investigation into the Structural Stability of Mixed-Halide Organic-Inorganic Perovskites, 2017. https://doi.org/10.13140/RG.2.2.25073.58727.

(8) Sebastian, M. T. Chapter Six - ABO_3 Type Perovskites. In *Dielectric Materials for Wireless Communication*; SEBASTIAN, M. T., Ed.; Elsevier: Amsterdam, **2008**; pp 161–203. https://doi.org/https://doi.org/10.1016/B978-0-08-045330-9.00006-6.

(9) Ye, W. N.; Xiong, Y. Review of Silicon Photonics: History and Recent Advances. *J. Mod. Opt.* **2013**, *60* (16), 1299–1320. https://doi.org/10.1080/09500340.2013.839836.

(10) Bello, S.; Urwick, A.; Bastianini, F.; Nedoma, A. J.; Dunbar, A. An Introduction to Perovskites for Solar Cells and Their Characterisation. *Energy Reports* **2022**, *8*, 89–106. https://doi.org/https://doi.org/10.1016/j.egyr.2022.08.205.

(11) Tan, C.; Gan, Z.; Gao, X. Temperature and Stress Distribution in the SOI Structure during Fabrication. *Semiconductor Manufacturing, IEEE Transactions* **2003**, *16*, 314–318. https://doi.org/10.1109/TSM.2003.811886.

(12) Wu, P.; Ma, X.; Ji, J.; Ma, Y. Review on Life Cycle Assessment of Energy Payback of Solar Photovoltaic Systems and a Case Study. *Energy Procedia.* **2017**, *105*, 68–74. https://doi.org/https://doi.org/10.1016/j.egypro.2017.03.281.

(13) Unni Krishnan, Manjot Kaur, Manjeet Kumar, and Akshay Kumar "Factors affecting the stability of perovskite solar cells: a comprehensive review," *Journal of Photonics for Energy* 9(2), 021001 (27 April 2019). https://doi.org/10.1117/1.JPE.9.021001

(14) *Best Research-Cell Efficiency Chart | Photovoltaic Research | NREL*. https://www.nrel.gov/pv/cell-efficiency.html (accessed 2024-03-24).

(15) Burschka, J.; Pellet, N.; Moon, S.-J.; Humphry-Baker, R.; Gao, P.; Nazeeruddin, M. K.; Grätzel, M. Sequential Deposition as a Route to High-Performance Perovskite-Sensitized Solar Cells. *Nature* **2013**, *499* (7458), 316–319. https://doi.org/10.1038/nature12340.

(16) Lee, M. M.; Teuscher, J.; Miyasaka, T.; Murakami, T. N.; Snaith, H. J. Efficient Hybrid Solar Cells Based on Meso-Superstructured Organometal Halide Perovskites. *Science* **2012**, *338* (6107), 643–647. https://doi.org/10.1126/science.1228604.

(17) Kim, H.-S.; Lee, C.-R.; Im, J.-H.; Lee, K.-B.; Moehl, T.; Marchioro, A.; Moon, S.-J.; Humphry-Baker, R.; Yum, J.-H.; Moser, J. E.; Grätzel, M.; Park, N.-G. Lead Iodide Perovskite Sensitized All-Solid-State Submicron Thin Film Mesoscopic Solar Cell with Efficiency Exceeding 9%. *Sci. Rep.* **2012**, *2* (1), 591. https://doi.org/10.1038/srep00591.

(18) Kojima, A.; Teshima, K.; Shirai, Y.; Miyasaka, T. Organometal Halide Perovskites as Visible-Light Sensitizers for Photovoltaic Cells. *J. Am. Chem. Soc.* **2009**, *131* (17), 6050–6051. https://doi.org/10.1021/ja809598r.

(19) Brittman, S.; Adhyaksa, G.; Garnett, E. The Expanding World of Hybrid Perovskites: Materials Properties and Emerging Applications. *MRS Commun.* **2015**, *5*, 1–20. https://doi.org/10.1557/mrc.2015.6.

(20) Kim, J. Y.; Lee, J.-W.; Jung, H. S.; Shin, H.; Park, N.-G. High-Efficiency Perovskite Solar Cells. *Chem. Rev.* **2020**, *120* (15), 7867–7918. https://doi.org/10.1021/acs.chemrev.0c00107.

(21) Li, Z.; Klein, T. R.; Kim, D. H.; Yang, M.; Berry, J. J.; van Hest, M. F. A. M.; Zhu, K. Scalable Fabrication of Perovskite Solar Cells. *Nat. Rev. Mater.* **2018**, *3* (4), 18017. https://doi.org/10.1038/natrevmats.2018.17.

(22) Leijtens, T.; Prasanna, R.; Bush, K.; Eperon, G.; Raiford, J.; Gold-Parker, A.; Wolf, E.; Swifter, S.; Boyd, C.; Wang, H.-P.; Toney, M.; Bent, S.; Mcgehee, M. Tin-Lead Halide Perovskites with Improved Thermal and Air Stability for Efficient All-Perovskite Tandem Solar Cells. *Sustain. Energy Fuels* **2018**, *2*. https://doi.org/10.1039/C8SE00314A.

(23) Gholipour, S.; Saliba, M. Chapter 1 - Bandgap Tuning and Compositional Exchange for Lead Halide Perovskite Materials. In *Characterization Techniques for Perovskite Solar Cell Materials*; Pazoki, M., Hagfeldt, A., Edvinsson, T., Eds.; Micro and Nano Technologies; Elsevier, **2020**; pp 1–22. https://doi.org/https://doi.org/10.1016/B978-0-12-814727-6.00001-3.

(24) Lin, R.; Xu, J.; Wei, M.; Wang, Y.; Qin, Z.; Liu, Z.; Wu, J.; Xiao, K.; Chen, B.; Park, S. M.; Chen, G.; Atapattu, H. R.; Graham, K. R.; Xu, J.; Zhu, J.; Li, L.; Zhang, C.; Sargent, E. H.; Tan, H. All-Perovskite Tandem Solar Cells with Improved Grain Surface Passivation. *Nature* **2022**, *603* (7899), 73–78. https://doi.org/10.1038/s41586-021-04372-8.

(25) Poindexter, J. R.; Hoye, R. L. Z.; Nienhaus, L.; Kurchin, R. C.; Morishige, A. E.; Looney, E. E.; Osherov, A.; Correa-Baena, J.-P.; Lai, B.; Bulović, V.; Stevanović, V.; Bawendi, M. G.;

Buonassisi, T. High Tolerance to Iron Contamination in Lead Halide Perovskite Solar Cells. *ACS Nano* **2017**, *11* (7), 7101–7109. https://doi.org/10.1021/acsnano.7b02734.

(26) Zhao, X.; Park, N.-G. Stability Issues on Perovskite Solar Cells. *Photonics* **2015**, *2* (4), 1139–1151. https://doi.org/10.3390/photonics2041139.

(27) Chen, T.; Xie, J.; Gao, P. Ultraviolet Photocatalytic Degradation of Perovskite Solar Cells: Progress, Challenges, and Strategies. *Advanced Energy and Sustainability Research* **2022**, *3* (6), 2100218. https://doi.org/https://doi.org/10.1002/aesr.202100218.

(28) Chen, S.; Xiao, X.; Gu, H.; Huang, J. Iodine Reduction for Reproducible and High-Performance Perovskite Solar Cells and Modules. *Sci. Adv.* **2021**, *7* (10), eabe8130. https://doi.org/10.1126/sciadv.abe8130.

(29) Masi, S.; Gualdrón-Reyes, A. F.; Mora-Seró, I. Stabilization of Black Perovskite Phase in FAPbI3 and CsPbI3. *ACS Energy Lett.* **2020**, *5* (6), 1974–1985. https://doi.org/10.1021/acsenergylett.0c00801.

(30) Kim, B.; Kim, J.; Park, N. First-Principles Identification of the Charge-Shifting Mechanism and Ferroelectricity in Hybrid Halide Perovskites. *Sci. Rep.* **2020**, *10*. https://doi.org/10.1038/s41598-020-76742-7.

(31) Gao, L.; Zhang, F.; Chen, X.; Xiao, C.; Larson, B. W.; Dunfield, S. P.; Berry, J. J.; Zhu, K. Enhanced Charge Transport by Incorporating Formamidinium and Cesium Cations into Two-Dimensional Perovskite Solar Cells. *Angewandte Chemie International Edition* **2019**, *58* (34), 11737–11741. https://doi.org/https://doi.org/10.1002/anie.201905690.

(32) Juarez-Perez, E. J.; Ono, L. K.; Uriarte, I.; Cocinero, E. J.; Qi, Y. Degradation Mechanism and Relative Stability of Methylammonium Halide Based Perovskites Analyzed on the Basis of Acid–Base Theory. *ACS Appl. Mater. Interfaces* **2019**, *11* (13), 12586–12593. https://doi.org/10.1021/acsami.9b02374.

(33) O'Kane, M. E.; Smith, J. A.; Alanazi, T. I.; Cassella, E. J.; Game, O.; van Meurs, S.; Lidzey, D. G. Perovskites on Ice: An Additive-Free Approach to Increase the Shelf-Life of Triple-Cation Perovskite Precursor Solutions. *ChemSusChem* **2021**, *14* (12), 2537–2546. https://doi.org/https://doi.org/10.1002/cssc.202100332.

(34) Meng, L.; Wei, Q.; Yang, Z.; Yang, D.; Feng, J.; Ren, X.; Liu, Y.; Liu, S. (Frank). Improved Perovskite Solar Cell Efficiency by Tuning the Colloidal Size and Free Ion Concentration in Precursor Solution Using Formic Acid Additive. *Journal of Energy Chemistry* **2020**, *41*, 43–51. https://doi.org/https://doi.org/10.1016/j.jechem.2019.04.019.

(35) Juarez-Perez, E. J.; Ono, L. K.; Qi, Y. Thermal Degradation of Formamidinium Based Lead Halide Perovskites into Sym-Triazine and Hydrogen Cyanide Observed by Coupled Thermogravimetry-Mass Spectrometry Analysis. *J. Mater. Chem. A* **2019**, *7* (28), 16912–16919. https://doi.org/10.1039/C9TA06058H.

(36) Yang, M.; Li, Z.; Reese, M. O.; Reid, O. G.; Kim, D. H.; Siol, S.; Klein, T. R.; Yan, Y.; Berry, J. J.; van Hest, M. F. A. M.; Zhu, K. Perovskite Ink with Wide Processing Window for Scalable High-Efficiency Solar Cells. *Nat. Energy* **2017**, *2* (5), 17038. https://doi.org/10.1038/nenergy.2017.38.

(37) Su, J.; Cai, H.; Yang, J.; Ye, X.; Han, R.; Ni, J.; Li, J.; Zhang, J. Perovskite Ink with an Ultrawide Processing Window for Efficient and Scalable Perovskite Solar Cells in Ambient Air. *ACS Appl. Mater. Interfaces* **2020**, *12* (3), 3531–3538. https://doi.org/10.1021/acsami.9b17141.

(38) Marques, A. S.; Faria, R. M.; Freitas, J. N.; Nogueira, A. F. Low-Temperature Blade-Coated Perovskite Solar Cells. *Ind. Eng. Chem. Res.* **2021**, *60* (19), 7145–7154. https://doi.org/10.1021/acs.iecr.1c00789.

(39) Yoo, J. W.; Jang, J.; Kim, U.; Lee, Y.; Ji, S.-G.; Noh, E.; Hong, S.; Choi, M.; Seok, S. Il. Efficient Perovskite Solar Mini-Modules Fabricated via Bar-Coating Using 2-Methoxyethanol-Based Formamidinium Lead Tri-Iodide Precursor Solution. *Joule* **2021**, *5* (9), 2420–2436. https://doi.org/https://doi.org/10.1016/j.joule.2021.08.005.

(40) Lee, J.-W.; Dai, Z.; Lee, C.; Lee, H. M.; Han, T.-H.; De Marco, N.; Lin, O.; Choi, C. S.; Dunn, B.; Koh, J.; Di Carlo, D.; Ko, J. H.; Maynard, H. D.; Yang, Y. Tuning Molecular Interactions for Highly Reproducible and Efficient Formamidinium Perovskite Solar Cells via Adduct Approach. *J. Am. Chem. Soc.* **2018**, *140* (20), 6317–6324. https://doi.org/10.1021/jacs.8b01037.

(41) Ahn, N.; Son, D.-Y.; Jang, I.-H.; Kang, S. M.; Choi, M.; Park, N.-G. Highly Reproducible Perovskite Solar Cells with Average Efficiency of 18.3% and Best Efficiency of 19.7% Fabricated via Lewis Base Adduct of Lead(II) Iodide. *J. Am. Chem. Soc.* **2015**, *137* (27), 8696–8699. https://doi.org/10.1021/jacs.5b04930.

(42) Saliba, M.; Matsui, T.; Seo, J.-Y.; Domanski, K.; Correa-Baena, J.-P.; Nazeeruddin, M. K.; Zakeeruddin, S. M.; Tress, W.; Abate, A.; Hagfeldt, A.; Gratzel, M. Cesium-Containing Triple Cation Perovskite Solar Cells: Improved, Reproducibility and High Efficiency. *Energy Environ. Sci.* **2016**, *9* (6), 1989–1997. https://doi.org/10.1039/c5ee03874j.

(43) Moloney, E. G.; Thrithamarassery Gangadharan, D.; Yeddu, V.; Zhang, D.; Moradi, S.; Askar, A. M.; Adachi, M. M.; Leitch, D. C.; Saidaminov, M. I. Inhibition of Amine–Water Proton Exchange Stabilizes Perovskite Ink for Scalable Solar Cell Fabrication. *Chemistry of Materials* **2022**, *34* (10), 4394–4402. https://doi.org/10.1021/acs.chemmater.1c04438.

(44) Bi, L.; Fu, Q.; Zeng, Z.; Wang, Y.; Lin, F. R.; Cheng, Y.; Yip, H.-L.; Tsang, S. W.; Jen, A. K.-Y. Deciphering the Roles of MA-Based Volatile Additives for α-FAPbI3 to Enable Efficient Inverted Perovskite Solar Cells. *J. Am. Chem. Soc.* **2023**, *145* (10), 5920–5929. https://doi.org/10.1021/jacs.2c13566.

(45) Salim, K. M. M.; Masi, S.; Gualdrón-Reyes, A. F.; Sánchez, R. S.; Barea, E. M.; Krecmarová, M.; Sánchez-Royo, J. F.; Mora-Seró, I. Boosting Long-Term Stability of Pure Formamidinium Perovskite Solar Cells by Ambient Air Additive Assisted Fabrication. *ACS Energy Lett.* **2021**, *6* (10), 3511–3521. https://doi.org/10.1021/acsenergylett.1c01311.

(46) Zhan占, Y.; Chen, W.; Yang, F.; Li李, Y. Stabilization of Formamidinium Lead Iodide Perovskite Precursor Solution for Blade-Coating Efficient Carbon Electrode Perovskite Solar Cells*. *Chinese Physics B* **2021**, *30*, 088803. https://doi.org/10.1088/1674-1056/abfbcb.

(47) Zhang, Y.; Xing, Z.; Fan, B.; Ni, Z.; Wang, F.; Hu, X.; Chen, Y. Uncovering Aging Chemistry of Perovskite Precursor Solutions and Anti-Aging Mechanism of Additives. *Angewandte Chemie International Edition* **2023**, *62* (8), e202215799. https://doi.org/https://doi.org/10.1002/anie.202215799.

(48) Chen, L.; Hu, M.; Lee, S.; Kim, J.; Zhao, Z.-Y.; Han, S.-P.; Lah, M. S.; Seok, S. Il. Deciphering Reaction Products in Formamidine-Based Perovskites with Methylammonium Chloride Additive. *J. Am. Chem. Soc.* **2023**, *145* (50), 27900–27910. https://doi.org/10.1021/jacs.3c12755.

(49) Liu, Y.; Sun, H.; Liao, F.; Li, G.; Zhao, C.; Cui, C.; Mei, J.; Zhao, Y. Bridging Effects of Sulfur Anions at Titanium Oxide and Perovskite Interfaces on Interfacial Defect Passivation and Performance Enhancement of Perovskite Solar Cells. *ACS Omega* **2021**, *6* (50), 34485–34493. https://doi.org/10.1021/acsomega.1c04685.

(50) Min, H.; Kim, G.; Paik, M. J.; Lee, S.; Yang, W. S.; Ung, M.; Seok, S. Il. Stabilization of Precursor Solution and Perovskite Layer by Addition Of. *Adv. Energy Mater.* **2019**, *9* (17). https://doi.org/10.1002/aenm.201803476.

(51) Chao, L.; Niu, T.; Gao, W.; Ran, C.; Song, L.; Chen, Y.; Huang, W. Solvent Engineering of the Precursor Solution toward Large-Area Production of Perovskite Solar Cells. *Advanced Materials* **2021**, *33* (14), 2005410. https://doi.org/https://doi.org/10.1002/adma.202005410.

(52) Hendriks, K. H.; van Franeker, J. J.; Bruijnaers, B. J.; Anta, J. A.; Wienk, M. M.; Janssen, R. A. J. 2-Methoxyethanol as a New Solvent for Processing Methylammonium Lead Halide Perovskite Solar Cells. *J. Mater. Chem. A* **2017**, *5* (5), 2346–2354. https://doi.org/10.1039/C6TA09125C.

(53) Lee, J.-W.; Kim, D.-H.; Kim, H.-S.; Seo, S.-W.; Cho, S. M.; Park, N.-G. Formamidinium and Cesium Hybridization for Photo- and Moisture-Stable Perovskite Solar Cell. *Adv. Energy Mater.* **2015**, *5* (20), 1501310. https://doi.org/https://doi.org/10.1002/aenm.201501310.

(54) Turren-Cruz, S.-H.; Hagfeldt, A.; Saliba, M. Methylammonium-Free, High-Performance, and Stable Perovskite Solar Cells on a Planar Architecture. *Science* **2018**, *362* (6413), 449–453. https://doi.org/10.1126/science.aat3583.

(55) Conings, B.; Drijkoningen, J.; Gauquelin, N.; Babayigit, A.; D'Haen, J.; D'Olieslaeger, L.; Ethirajan, A.; Verbeeck, J.; Manca, J.; Mosconi, E.; Angelis, F. De; Boyen, H.-G. Intrinsic Thermal Instability of Methylammonium Lead Trihalide Perovskite. *Adv. Energy Mater.* **2015**, *5* (15), 1500477. https://doi.org/https://doi.org/10.1002/aenm.201500477.

(56) Rizzo, A.; Listorti, A.; Colella, S. Chemical Insights into Perovskite Ink Stability. *Chem.* **2022**, *8* (1), 31–45. https://doi.org/https://doi.org/10.1016/j.chempr.2021.11.004.

(57) Valenzano, V.; Cesari, A.; Balzano, F.; Milella, A.; Fracassi, F.; Listorti, A.; Gigli, G.; Rizzo, A.; Uccello-Barretta, G.; Colella, S. Methylammonium-Formamidinium Reactivity in Aged Organometal Halide Perovskite Inks. *Cell Rep. Phys. Sci.* **2021**, *2* (5), 100432. https://doi.org/https://doi.org/10.1016/j.xcrp.2021.100432.

(58) Chen, C.; Rao, Y.; Li, Z.; Wang, X.; Cui, G.; Wang, W.; Pang, S. Stabilizing Formamidinium Lead Iodide Perovskite Precursor Solution with Phenylboric Acid. *Solar RRL* **2021**, *5* (3), 2000715. https://doi.org/https://doi.org/10.1002/solr.202000715.

(59) Castriotta, L. A.; Calabrò, E.; Di Giacomo, F.; Reddy, S. H.; Takhellambam, D.; Paci, B.; Generosi, A.; Serenelli, L.; Menchini, F.; Martini, L.; Tucci, M.; Di Carlo, A. A Universal Multi-Additive Strategy to Enhance Efficiency and Stability in Inverted Perovskite Solar Cells. *Nano Energy* **2023**, *109*, 108268. https://doi.org/https://doi.org/10.1016/j.nanoen.2023.108268.

(60) Zhou, T.; Chen, J.; Kuang, A. Inhibiting the Decomposition of Methylammonium Using Cations with Low Deprotonation Energy. *J. Mater. Chem. A* **2022**, *10* (42), 22742–22749. https://doi.org/10.1039/D2TA05753K.

(61) National Center for Biotechnology Information. *PubChem Compound Summary for CID 8019, 2-Methoxyethanol.* Pubchem.

(62) Fitzpatrick, P. F.; Villafranca, J. J. The Mechanism of Inactivation of Dopamine β-Hydroxylase by Hydrazines. *Journal of Biological Chemistry* **1986**, *261*, 4510–4518.

(63) Kovalenko, A.; Hrabal, M. Printable Solar Cells. In *Printable Solar Cells*; 2017; pp 163–202. https://doi.org/10.1002/9781119283720.ch5.

(64) Stuhrmann, B. Self-Organized Active Biopolymer Networks in Migrating Living Cells, 2009.

(65) Van Gompel, W. T. M.; Herckens, R.; Reekmans, G.; Ruttens, B.; D'Haen, J.; Adriaensens, P.; Lutsen, L.; Vanderzande, D. Degradation of the Formamidinium Cation and the Quantification of the Formamidinium–Methylammonium Ratio in Lead Iodide Hybrid Perovskites by Nuclear Magnetic Resonance Spectroscopy. *The Journal of Physical Chemistry C* **2018**, *122* (8), 4117–4124. https://doi.org/10.1021/acs.jpcc.7b09805.

(66) Dooley David M. and Brown, D. E. and M. M. A. and S. L. J. Mechanistic Studies of Copper/Topa Amine Oxidases. In *Biochemistry of Vitamin B6 and PQQ*; Marino G. and Sannia, G. and B. F., Ed.; Birkhäuser Basel: Basel, 1994; pp 253–257.

(67) Kirmse, W. Nitrogen as Leaving Group: Aliphatic Diazonium Ions. *Angewandte Chemie International Edition in English* **1976**, *15* (5), 251–261. https://doi.org/https://doi.org/10.1002/anie.197602511.

(68) Zollinger, H. Nitrogen as Leaving Group: Dediazoniations of Aromatic Diazonium Ions. *Angewandte Chemie International Edition in English* **1978**, *17* (3), 141–150. https://doi.org/https://doi.org/10.1002/anie.197801413.

(69) Ellson, B. S. P. R.; Stearns, B. S. P. R.; Mutz, B. S. P. M.; Brown, B. S. P. C.; Browning, B. S. P. B.; Harris, B. S. P. D.; Qureshi, B. S. P. S.; Shieh, B. S. P. J.; Wold, B. S. P. D. In Situ DMSO Hydration Measurements of HTS Compound Libraries. *Comb. Chem. High Throughput Screen* **2005**, *8 6*, 489–498.

(70) Aydin, E.; De Bastiani, M.; De Wolf, S. Defect and Contact Passivation for Perovskite Solar Cells. *Adv. Mat.* **2019**, *31* (25), 1900428. https://doi.org/https://doi.org/10.1002/adma.201900428.

(71) Jiang, Q.; Tong, J.; Xian, Y.; Kerner, R. A.; Dunfield, S. P.; Xiao, C.; Scheidt, R. A.; Kuciauskas, D.; Wang, X.; Hautzinger, M. P.; Tirawat, R.; Beard, M. C.; Fenning, D. P.; Berry, J. J.; Larson, B. W.; Yan, Y.; Zhu, K. Surface Reaction for Efficient and Stable Inverted Perovskite Solar Cells. *Nature* **2022**, *611* (7935), 278–283. https://doi.org/10.1038/s41586-022-05268-x.

Appendix: Contributions

First-authored papers:

- Sean Reinecke, Vishal Yeddu, Dongyang Zhang, Chris Barr, Jeremy E. Wulff, Sergey V. Dayneko, Mohammad Reza Kokaba, Makhsud I. Saidaminov. "Multiple Stabilization Effects of Benzylhydrazine on Scalable Perovskite Precursor Inks". Under review. *The paper has multi-author contributors. I have contributed to planning experiments, performing the ink NMR and XRD experiments, as well as the bulk of the analysis, writing, and editing.*

Co-authored papers:

- Dongyang Zhang, Sutripto Khasnabis, Wanlong Wang, Vishal Yeddu, Shahram Moradi, Muhammad Awais, Hai-Dang Nguyen, **Sean B. Reinecke**, Yuki Haruta, Robert Godin, Furui Tan, Makhsud I. Saidaminov. "Cadmium-Doping Slows Trap Emptying in Ambient-Air Blade-Coated Formamidinium Lead Iodide Perovskite Solar Cells". Advanced Energy Materials (2024). *I have contributed to editing this paper.*
- Yu Li, Shanshan Yu, Junjie Yang, Kai Zhang, Mingyu Hu, Weitao Qiu, Fumin Guo, Wei Qian, **Sean Reinecke**, Tao Chen, Makhsud I. Saidaminov, Jian Wang, Shihe Yang. "Filterless narrowband photodetectors enabled by controllable band modulation through ion migration: The case of halide perovskites". InfoMat (2024) 6(1) e12506. *I have contributed to editing this paper.*
- Mohammad Reza Kokaba, Yameen Ahmed, Vishal Yeddu, Dongyang Zhang, Parinaz Moazzezi, Vahid Kamraninejad, Sergey Dayneko, **Sean B. Reinecke**, Augusto Amaro, Bohores Villarejo, Anjusree Shyla, Sardar Malek, Makhsud I. Saidaminov. "Enhanced Particle-to-Particle Interaction of Tin Oxide Electron Transporter Layer for Scalable Flexible Perovskite Solar Cells". Solar RRL (2024) 2301013. *I have contributed to NMR instrumentation work and editing this paper.*